Small-Angle X-Ray Scattering Studies on Cytochrome Oxidases and Amylases

（X線小角散乱法によるチトクロム酸化酵素及びアミラーゼの構造研究）

A Doctoral Thesis
submitted by
Mamoru Sato
to
Faculty of Engineering
Osaka University
1983

ACKNOWLEDGEMENTS

First of all, it should be mentioned that the work of this thesis has been carried out under the guidance of Professor Nobutami Kasai in collaboration with Professor Masao Kakudo's group of Institute for Protein Research, Osaka University.

The author is greatly indebted to Professor Nobutami Kasai for his cordial guidance, advice and encouragement throughout this investigation.

The author is greatly indebted to Professor Masao Kakudo for his continuous guidance and encouragement.

The author is deeply indebted to Dr. Nobuo Tanaka for his continuous guidance and helpful advice throughout this investigation.

The author expresses his great gratitude to Professor Takayuki Ozawa and Dr. Masashi Tanaka of Department of Biomedical Chemistry, Faculty of Medicine, University of Nagoya, for their useful discussion and biochemical advices for cytochrome oxidase from beef heart.

The author expresses his deep gratitute to Professor Tateo Yamanaka and Dr. Yoshihiro Fukumori of Department of Chemistry, Faculty of Science, Tokyo Institute of Technology, for their useful discussion and biochemical advices for cytochrome oxidase from *Nitrobacter agilis*.

The author expresses his great thank to Professor Tokuya Harada, Institute of Scientific and Industrial Research, Osaka University for his useful discussion and biochemical advice for

Pseudomonas isoamylase.

The author expresses his deep thank to Dr. Kinji Kakiuchi of Institute for Protein Research, Osaka University for measurement by analytical ultracentrifugation.

The author wishes to thank Dr. Yasushi Kai, Dr. Kunio Miki and Dr. Shigeharu Harada for their kind assistance and encouragement.

The author is grateful to Dr. Noritake Yasuoka of Institute for Protein Research, Osaka University for utilization of ACOS 700 computer.

The author is also grateful to Dr. Yasuo Hata and Miss Sachiko Bando of Institute for Protein Research, Osaka University for their kind assistance and encouragement.

Thanks are given to Miss Nobuko Kanehisa and Mr. Mitsunori Kato for their kind assistance.

Finally, the author would like to acknowledge all members of Kasai laboratory and Kakudo laboratory for their friendships.

CONTENTS

LIST OF ABBREVIATIONS

PSPC	position-sensitive proportional counter
$\tilde{I}$	smeared scattering intensity
I	desmeared scattering intensity
s	scattering parameter ($s = 4\pi\sin\theta/\lambda$)
2θ	scattering angle
λ	wavelength
R_{sym}	reliablity factor
$P(r)$	distance distribution function
$D\text{-}P(r)$	difference distance distribution function
R_g	radius of gyration
D_{max}	maximal dimension
r_{max}	r where $P(r)$ peaks
V	volume
M_r	molecular weight
$\overline{v}$	partial specific volume
$s_{20,w}$	sedimentation coefficient in water at 20 °C
DOC	deoxycholate
AS	ammonium sulfate
sup	supernatant
ppt	precipitate
CMC	critical micelle concentration
SDS	sodium dodecyl sulfate

GENERAL INTRODUCTION

Small-angle X-ray scattering method gives structural information from the intensity distribution scattered near the incident X-ray beam. The structural information derived from this method is less than that derived from X-ray crystallographic analysis, which presents the detailed information about the structure at almost atomic level. However, the recent developments of the X-ray source such as synchrotron orbital radiation and one- or two-dimensional counter greatly shortened the measurement of the scattering intensities enough to dynamically detect the structural changes of some biological macromolecules. It was consequentially made possible to study the structure and function relationship of the macromolecule in solution by utilization of the small-angle X-ray scattering method. In this way, the small-angle X-ray scattering method presents the structural information more correlative with the biological system than that derived from the X-ray crystallographic analysis, and became to the most useful technique in studying the relationship between the structure of the biological macromolecule and the function.

In the present thesis, I have dealed with the enzymes concerned to some biologically important system and investigated the structure and its relation with the function by small-angle X-ray scattering method. CHAPTER I dealed with the small-angle X-ray scattering system that I have developed for the purpose of shortening of measurement and some new treatments of the small-angle X-ray scattering intensity data. In CHAPTER II

and CHAPTER III, the structures of cytochrome aa_3-type oxidase from beef heart mitochondria and *Nitrobacter agilis* were discussed, respectively. In CHAPTER IV, the structures of Taka-amylase A and *Pseudomonas* isoamylase in solution and in crystal were discussed. Finally in appendix, the survey of small-angle X-ray scattering theory used in this investigation was introduced.

CHAPTER I

Developments of Small-Angle X-Ray Scattering System And New Treatments of Small-Angle X-Ray Scattering Data

1. Small-Angle X-Ray Scattering System

The schematic drawing of the small-angle X-ray scattering system that I have developed for the purpose of shortening of measurement is shown in Fig. I-1. The X-ray source is 0.1 x 0.1 mm spot (foreshortened to 0.1 x 0.1 mm at a glancing angle of 6°) on the copper anode of a Regaku fine focus rotating-anode X-ray generator (FR-B) operated at 50 KV, 70 mA (9 000 rpm). The nickel filtered (10 μm in thickness) X-ray beams are reflected and focussed by a nickel-coated bent glass mirror through two kinds of appropriate limiting slits, the first slit used for the adjustment of the width and the length of incident X-ray beam and the second for the removal of the parasitic scattering from the edges of the first slit.

The small-angle X-ray scattering intensities are recorded on a position-sensitive proportional counter, PSPC (1) (the flowing gas is 90% argon and 10% methane, in thickness of 11 mm). The sample is sucked into a thin-walled quartz capillary settled in the sample holder by the injector connected at the top of the capillary through a tigon tube. This system needs only 10 μl of solution per measurement and can give a meaningful scattering intensity distribution in the range of scattering angles, 2θ = 4.0 - 76.7 mrad, corresponding to Bragg spacings of 400 - 20 Å, with 15 - 180 min accumulation of the

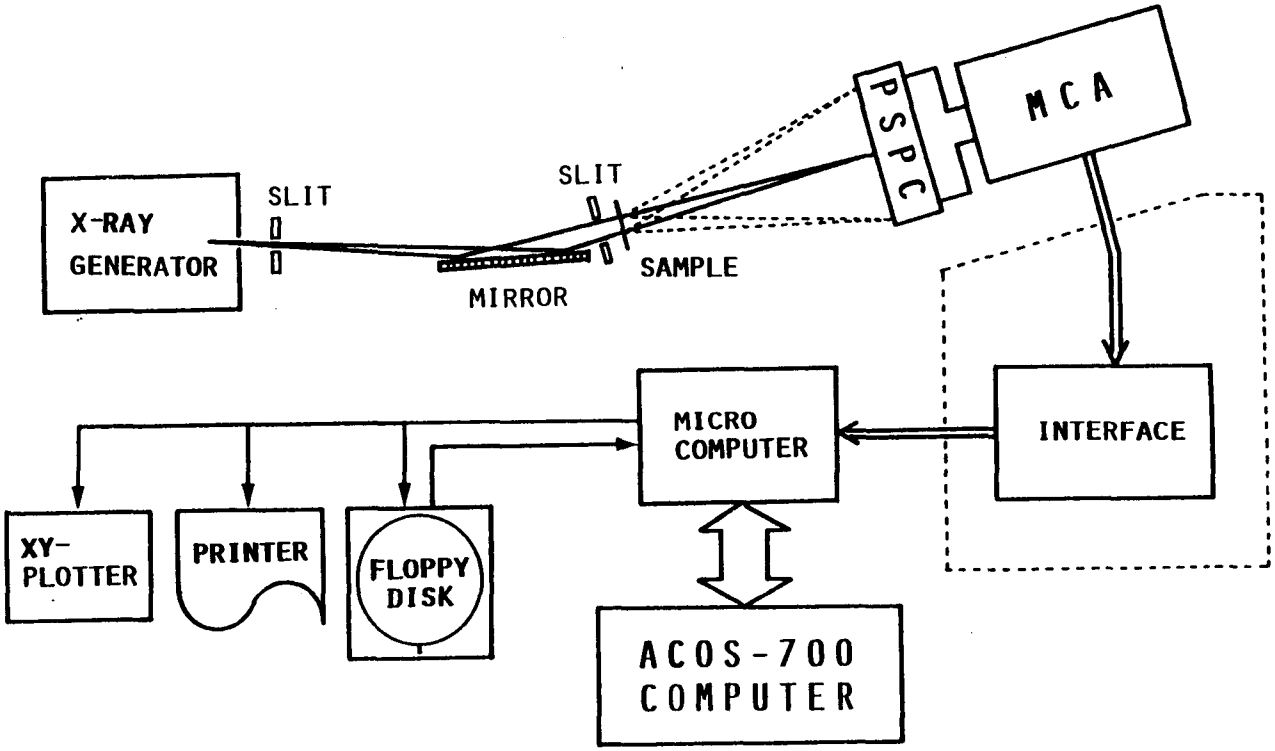

Fig. I-1. Schematic drawing of small-angle X-ray scattering system. PSPC : position-sensitive proportional counter. MCA : multi-channel analyzer.

scattering intensities. The distance between the sample and the counter is calibrated from the powder diffraction of sodium myristate.

The small-angle X-ray scattering system is controled by a micro-computer. Small-angle X-ray scattering intensities recorded on the PSPC are stored in process memory through multi-channel analyzer, and are transmitted immediately to the micro-computer through an interface. The scattering intensity data thus transmitted are then saved in a flopy disk, and are processed or analyzed with the micro-computer and an ACOS 700 computer, which are connected with each other by a RS 232C circuit. Programmes developed for the process and the analysis of the scattering intensity data are listed in Table I-1.

Table I-1. Programmes developed for the process and the analsis of small-angle X-ray scattering intensity data

Programme Name	Function
PROX	Transmission of measured small-angle X-ray scattering intensities from PSPC to micro-computer
ATSS	Transmission of various kinds of data from micro-computer to ACOS 700 computer or from ACOS 700 computer to micro-computer
AVERAGE	Subtraction of background intensities, correction for the sensitivity of PSPC and averaging of equivalent scattering intensities
DESMEAR	Desmearing of smeared scattering intensities
GUINIER	Guinier plot of scattering intensities
PR	Calculation of distance distribution function, $P(r)$
DEL-PR	Calculation of difference distance distribution function, D-$P(r)$
VOLUME	Calculation of particle volume
ELLIPSOID	Least-squares fitting between observed scattering intensities and theoretical scattering intensities from an ellipsoid of revolution
SPHERE	Least-squares fitting between observed scattering intensities and theoretical scattering intensities from sphere
PLOTTING	Plotting of various kinds of data by X-Y plotter

2. Data Processing of Small-Angle X-Ray Scattering Intensities

Data processing procedure of small-angle X-ray scattering intensities is summarized in Table I-2. The scattering intensities recorded on both sides of the direct X-ray beam are corrected for the sensitivity of the PSPC, from which the background intensities are subtracted. The center of the direct X-ray beam (zero angle) is then precisely searched so as to realize the best coincidence of the scattering intensities at equivalent positions on the both sides of the zero angle. The coincidence is expressed by a reliablity factor, R_{sym} ;

$$R_{sym} = \left[\frac{\sum_{i=1}^{N} (I_i - I_i')^2}{\sum_{i=1}^{N} \bar{I}_i^2} \right]^{1/2}$$

where I_i and I_i' are i-th equivalent scattering intensities on both sides of the direct X-ray beam, respectively, $\bar{I}_i$ the average of I_i and I_i', and N the number of the equivalent scattering intensities. The independent scattering intensities are then obtained by correcting for a collimation effect (desmearing, see 3).

The scattering parameters, s is defined by $s = 4\pi\sin\theta/\lambda$, where 2θ is the scattering angle and λ the wavelength (λ = 1.5418 Å).

Table I-2. Data processing procedure of small-angle X-ray scattering intensities

Small-angle X-ray scattering intensities recorded on both sides of a direct X-ray beam
↓
Correction for the sensitivity of PSPC
↓
Subtration of background intensities
↓
Searching of the position of the direct X-ray beam so as to minimize a reliability factor
↓
Averaging of the equivalent scattering intensities
↓
Correction for a collimation effect
↓
Independent scattering intensities, $I(s)$

3. Correction for Collimation Effect (Desmearing)

In order to obtain sufficient scattering intensity distribution in small-angle X-ray scattering experiment, a slit collimation system is normally used. Small-angle X-ray scattering intensities obtained by the slit collimation are not those obtained by a pinhole collimation with an infinitely small

window counter but are the pinhole scattering intensities averaged over an angular range which is defined by the geometry of the slit collimation.

The effect by the slit collimation can be split into slit length and slit width effects (2). The scattering intensities (smeared scattering intensities), $\tilde{I}(s)$, which is experimentally measured by the slit collimation, are given by the convolution of $P(t)$, $Q(x)$ and $I(s)$ as (2)

$$\tilde{I}(s) = 2 \int_0^\infty dt \int_{-\infty}^{\infty} P(t)\ Q(x)\ I[((\ s - x\ )^2 + t^2\ )^{1/2}]\ dx \qquad \text{----------[I-1]}$$

where $P(t)$ and $Q(x)$ are slit length and slit width functions, respectively, which are normalized so that

$$2 \int_0^\infty P(t)\ dt = \int_{-\infty}^{\infty} Q(x)\ dx$$

$I(s)$ is practically required for the structural analysis by small-angle X-ray scattering method, and is obtained by the deconvolution of $\tilde{I}(s)$ (desmearing).

Guinier and Fournet (3), and DuMond (4) solved the equation [I-1] for the collimation system of infinitely high and negligibly narrow slits. Their method was modified by Kratky *et al.* (5) for use with certain types of finite slit length collimation. These methods needs to measure the intensity distribution of incident X-rays. On the other hand, Lake (6) has reported an iterative method for solving the equation [I-1] without measurement of the distribution. However, the recent development of a computer made it possible to solve the equation

[I-1] directly. The method is mentioned below.

METHOD

I) *Principle*

The method is applied on the following three assumptions.

1. Slit width effect is taken no account, that is, negligibly narrow slit.
2. The focus size on the target of X-ray generator is infinitely small.
3. X-ray phtons incident to the position between the channel and the neighbor channel are distributed proportionally to depend on the position-channel and position-neighbor channel distances.

The collimation geometry applied on this method is presented in Fig. I-2. The intensity, $dI(t,z)$ that the X-ray photons incident to the sample at the height, z give to PSPC at the height, t can be expressed as

$$dI(t,z) = I[((t - Dz)^2 + S_0^2)^{1/2}] \text{ ----------[I-2]}$$

where D is $(d_1 + d_2) / d_1$ (d_1 : focus-to-sample distance, d_2 : sample-to-counter distance) and S_0 defined in Fig. I-2.
The intensity observed at the point separated by S_0 from the center of the direct X-ray beam, $\tilde{I}(S_0)$ is given as

$$\tilde{I}(S_0) = \int_{-z_0}^{z_0} \int_{-x_0}^{x_0} dI(t,z)\, dt\, dz \text{ ----------[I-3]}$$

Substituted the equation [I-2] to the equation [I-3],

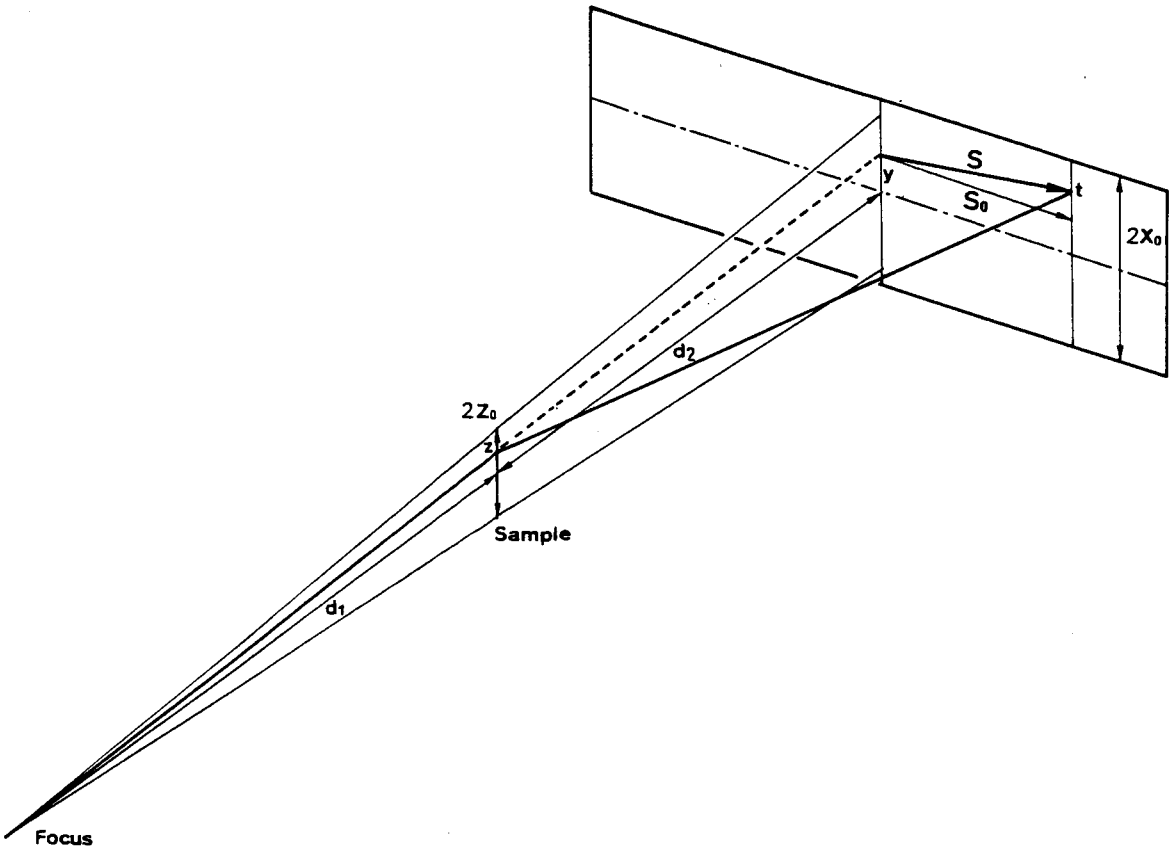

Fig. I-2. Collimation geometry

$$\tilde{I}(S_0) = \int_{-z_0}^{z_0} \int_{-x_0}^{x_0} I[((t - Dz)^2 + S_0^2)^{1/2}]\, dt\, dz$$

$$= \frac{1}{D} \int_{-Dz_0}^{Dz_0} \int_{-x_0}^{x_0} I[((t - Z)^2 + S_0^2)^{1/2}]\, dt\, dZ \quad \text{--[I-4]}$$

where $Z = Dz$

In the equation [I-4], $\tilde{I}$ and I are the scattering intensities before and after correction for a collimation effect, respectively ($\tilde{I}$: smeared scattering intensity, I : desmeared scattering intensity).

II) *Solution of equation [I-4]*

The integration of the equation is carried out numerically: N division of $2Dz_0$ and M division of $2x_0$, that is,

$$\tilde{I}(S_0) = \frac{2Dz_0}{N} \frac{2x_0}{M} \frac{1}{D} \sum_{n=1}^{N} \sum_{m=1}^{M} I(S) \quad \text{----------[I-5]}$$

where $S = [(t_0 - Z_0 - \frac{2x_0}{M}(m - 1) + \frac{2Dz_0}{N}(n - 1))^2 + S_0^2]^{1/2}$.

If $S_0 \geq S_i$ and $S_0 < S_{i+1}$ (S_i : distance between the center of the direct beam and i-th channel of PSPC), from the assumption 3, $\tilde{I}(S_0)$ is expressed by

$$\tilde{I}(S_0) = \frac{S_{i+1} - S_0}{S_{i+1} - S_i} \tilde{I}(S_i) + \frac{S_0 - S_i}{S_{i+1} - S_i} \tilde{I}(S_{i+1}) \quad \text{--[I-6]}$$

where $\tilde{I}(S_i)$ and $\tilde{I}(S_{i+1})$ are the smeared scattering intensities recorded at the i-th and $(i+1)$-th channels of PSPC, respectively. The substitution of the equation [I-6] to the equation [I-5] makes it possible to relate the smeared scattering intensities

with desmeared scattering intensities by a matrix, $\mathbf{M}$

$$\tilde{\mathbf{I}} = \mathbf{M} \times \mathbf{I} \qquad \text{----------[I-7]}$$

where $\tilde{\mathbf{I}}$ and $\mathbf{I}$ are one-dimensional matrixes of $\tilde{\mathbf{I}} = (\tilde{I}(S_1), \tilde{I}(S_2), \tilde{I}(S_3), \text{------}, \tilde{I}(S_n))$ and $\mathbf{I} = (I(S_1), I(S_2), I(S_3), \text{------}, I(S_n))$, respectively. Use of the inverse matrix of $\mathbf{M}$, $\mathbf{M}^{-1}$ gives the following matrix equation :

$$\mathbf{I} = \mathbf{M}^{-1} \times \tilde{\mathbf{I}} \qquad \text{----------[I-8]}$$

In this way, the desmeared scattering intensities are obtained directly from the equation [I-8], which are compared with the smeared scattering intensities in Fig. I-3.

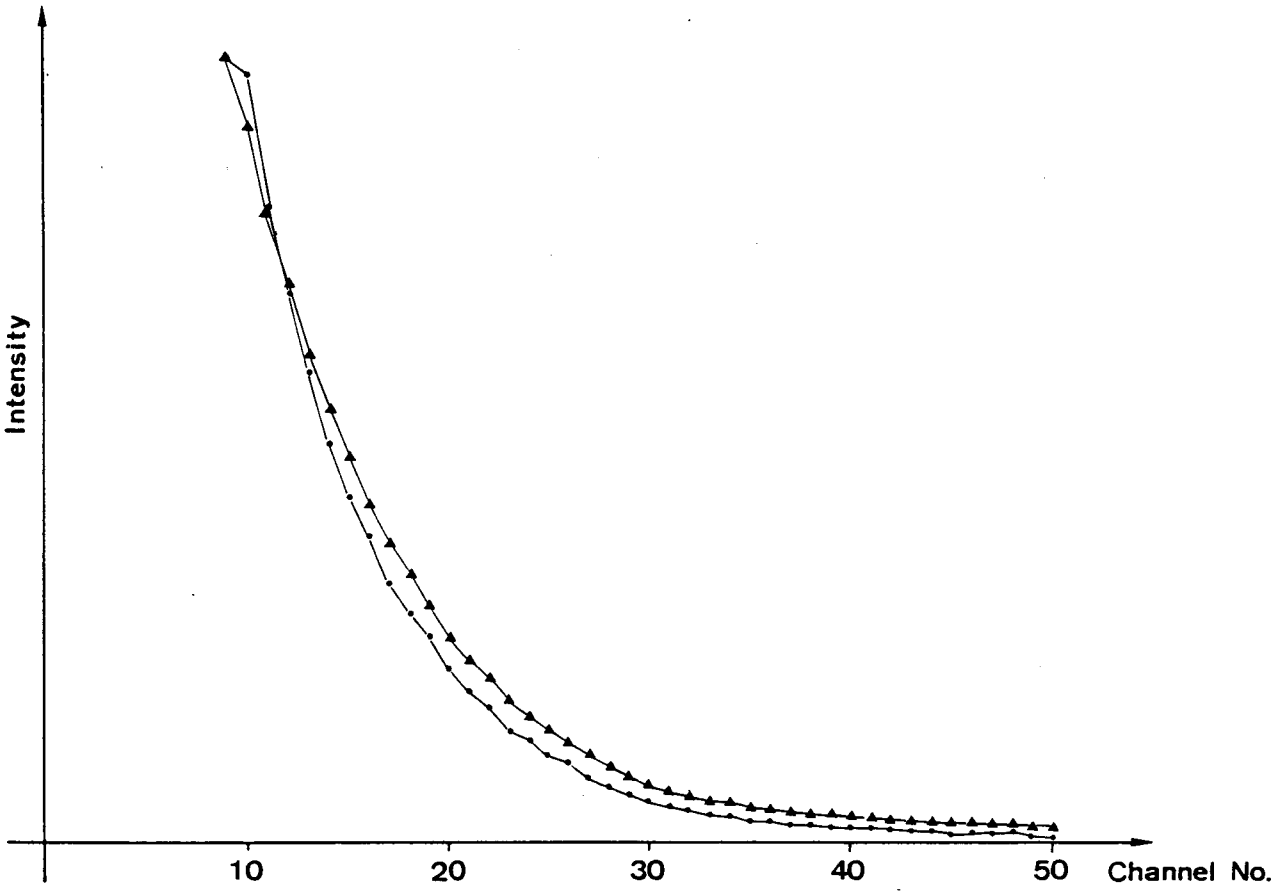

Fig. I-3. Smeared scattering intensity curve (—▲—) and desmeared scattering intensity curve (—●—)

CHAPTER II

Structural Studies on Cytochrome Oxidase Isolated from Beef Heart Mitochondria And The Complex with Cytochrome *c*

1. Introduction

Cytochrome oxidase (ferrocytochrome *c* : oxygen oxidoreductase EC 1.9.3.1) is the terminal component of electron-transfer chain in mitochondria of eukaryote and in plasma membrane of prokaryote. It catalyzes electron transfer from ferrocytochrome *c* to molecular oxygen and functions as an energy transducer which convents the energy of electron transfer to a driving force for ATP synthesis. Cytochrome oxidase isolated from beef heart mitochondria has a minimal molecular weight of about 130 000 and consists of three large hydrophobic and four small hydrophilic subunits containing two heme *a* groups (heme *a* and heme a_3) and two copper atoms. The oxidase is widely studied intrinsic membrane protein (7) and contains 20-30% (w/w) of phospholipids (8). In order to investigate the structure of the oxidase by means of small-angle X-ray scattering, it is prerequisite to remove phospholipids bound to the oxidase. Recently, Ozawa *et al.* have reported a procedure for purification of the oxidase by hydrophobic interaction chromatography with phenyl-Sepharose (7) and affinity chromatography with Sepharose-bound cytochrome *c* (9). By these chromatographic procedures, it became to be possible to obtain phospholipid-depleted preparation of the oxidase, which retains only 2 moles of tightly bound cardiolipin per mole of the oxidase (10).

Binding of cytochrome *c* to cytochrome oxidase has been proposed to control the rate of electron transport through the terminal segment of the respiratory chain in mitochondrial inner membrane (11). It is of great importance to determine the structures in solution of the oxidase and the complex with cytochrome *c*. In this chapter, the structures in solution of cytochrome oxidase isolated from beef heart mitochondria and the complex with cytochrome *c* have been investigated with the effect by ionic strength on the complex formation by means of small-angle x-ray scattering.

2. Experimental

Protein concentration was determined by biuret method (12) using bovine serum albumin as a standard. In order to correct the contribution of alkaline hemochromogen of heme *a* to absorbance at 540 nm, 0.6% sodium potassium tartarate tetrahydrate solution in 3% sodium hydroxide was used in place of biuret reagent. Heme *a* concentration was determined from the reduced spectrum using $\Delta\varepsilon_{605-630} = 16.5\ mM^{-1}cm^{-1}$ (13). Phosphorus was determined by the method of Chen *et al.* (14), and amount of phospholipids was calculated assuming their average molecular weight as 775.

Isolations and purifications of cytochrome oxidase and cytochrome c

Isolation and purification procedure of cytochrome oxidase is presented in Table II-1. Cytochrome oxidase was isolated from beef heart mitochondria according to the method of Fowler *et al.* (15), and was refractionated with ammonium sulfate in

Table II-1. Isolation and purification procedure of cytochrome oxidase

---

Beef heart
↓ Homogenized in a glass-Teflon homogenizer
↓ Suspended in 0.25 M sucrose solution
↓ Centrifuged at 105 000 x g for 20 min
ppt
↓ Suspended in 50 mM Tris-HCl buffer, pH 8.0, containing 0.66 M sucrose and 1 mM histidine
↓ + DOC (0.3 mg/mg protein)
↓ + KCl (72 g/l) and incubated for 15 min
↓ Centrifuged at 105 000 x g for 30 min
Green residue
↓ Washed with 2 volumes of 50 mM Tris-HCl buffer, pH 8.0, containing 0.66 M sucrose and 1 mM histidine
↓ Centrifuged at 105 000 x g for 20 min
Green pellet
↓ + DOC (0.5 mg/mg protein)
↓ + KCl (74.5 g/l)
↓ Centrifuged at 105 000 x g for 20 min
Green sup
↓ Dialyzed against 30 volumes of 10 mM Tris-HCl buffer, pH 8.0 for 90 min
↓ + 0.19 volume of sat. AS and incubated for 10 min
↓ Centrifuged at 105 000 x g for 20 min
sup
↓ + 0.04 volume of sat. AS and incubated for 10 min
↓ Centrifuged at 105 000 x g for 20 min
ppt
↓ Dissolved in 50 mM Tris-HCl buffer, pH 8.0 and adjusted the protein concentration to 20 - 30 mg/ml
↓ + 0.2586 volume of 20% cholate (3% cholate)
↓ + 0.4655 volume of sat. AS (27% sat.)
↓ Incubated at 4 °C for 4 h

Table II-1. (continued)

↓ Centrifuged at 78 000 x g for 10 min

sup

↓ Incubated for 2 h at 30 °C

↓ Centrifuged at 78 000 x g for 10 min

sup

↓ + equal volume of 50 mM Tris-HCl buffer, pH 8.0

↓ + 0.384 volume of sat. AS (37.5% sat.)

↓ Incubated for 2 h

↓ Centrifuged at 78 000 x g for 10 min

ppt

↓ Dissolved in 50 mM Tris-HCl buffer, pH 8.0

↓ + 0.5 volume of sat. AS (33% sat.)

↓ Centrifuged at 78 000 x g for 20 min

ppt

↓ Dissolved in 0.1 M sodium bicarbonate buffer, pH 8.3, containing 0.1 M NaCl and 1% DOC

↓ Charged onto phenyl-Sepharose CL-4B column (1 x 20 cm) equilibrated with 0.1 M sodium bicarbonate buffer, pH 8.3, containing 0.1 M NaCl and 1% DOC

↓ Washed with 500 ml of the equilibrium buffer

↓ Eluted with 0.1 M sodium bicarbonate buffer, pH 8.3, containing 0.1 M NaCl and 1% Triton X-100

↓ Diluted ten times with 10 mM Tris-HCl buffer, pH 7.5, containing 0.1% Triton X-100

↓ Charged onto cytochrome *c*-Sepharose 4B (1 x 20 cm) equilibrated with 10 mM Tris-HCl buffer, pH 7.5, containing 0.1% Triton X-100

↓ Washed with 50 ml of the equilibrium buffer

↓ Eluted with a linear gradient (0 - 0.2 M) of NaCl in total volume of 100 ml of the equilibrium buffer

↓ Charged onto Sephacryl S-400 column (1.5 x 116 cm) equilibrated with 0.1 M Tris-HCl buffer, pH 7.5, containing 0.5% cholate

Table II-1. (continued)

↓ Eluted with 0.1 M Tris-HCl buffer, pH 7.5, containing 0.5% chlate

↓

Purified cytochrome oxidase

---

sup : supernatant

ppt : precipitate

sat. AS : 100% saturated ammonium sulfate

DOC : deoxycholate

the presence of 3% cholate by the method of Tzagoloff and MacLennan (16). The refractionated oxidase was further purified by phenyl-Sepharose CL-4B hydrophobic chromatography (7) and cytochrome *c*-Sepharose 4B affinity chromatography (9). The oxidase was passed through a column of Sephacryl S-400 equilibrated with 0.1 M Tris-HCl buffer, pH 7.5, containing 0.5% cholate. The specific heme *a* content of the purified oxidase was 14.2 nmol/mg and its phospholipid content was 2.0% (w/w). The densitometric tracing of SDS polyacrylamide gel electrophoresis profile of the purified oxidase is shown in Fig. II-1.

Cytochrome *c* (isolated from horse heart), purchased from Sigma (Type III) was purified by the method of Hagihara *et al.* (17).

Preparation of samples for small-angle X-ray scattering intensity measurements

Cytochrome oxidase purified by the Sephacryl S-400 gel filtration was dialyzed against H_2O, containing 1% cholate. Cytochrome *c* was added to the oxidase solution in heme *c* : heme *a* ratio of 1 : 2 (1 : 1 mol/mol). The mixture solution was prepared to 120 μM in heme *a* with various concentrations of Tris-HCl buffer, pH 8.0, containing 1% cholate. The oxidase solution and cytochrome *c* solution were also prepared to 120 μM in heme *a* and 730 μM in heme *c* with various concentrations of Tris-HCl buffer, pH 8.0, containing 1% cholate, respectively.

Measurements of small-angle X-ray scattering intensities

The small-angle X-ray scattering intensities were measured on the system equipped with a position-sensitive proportional

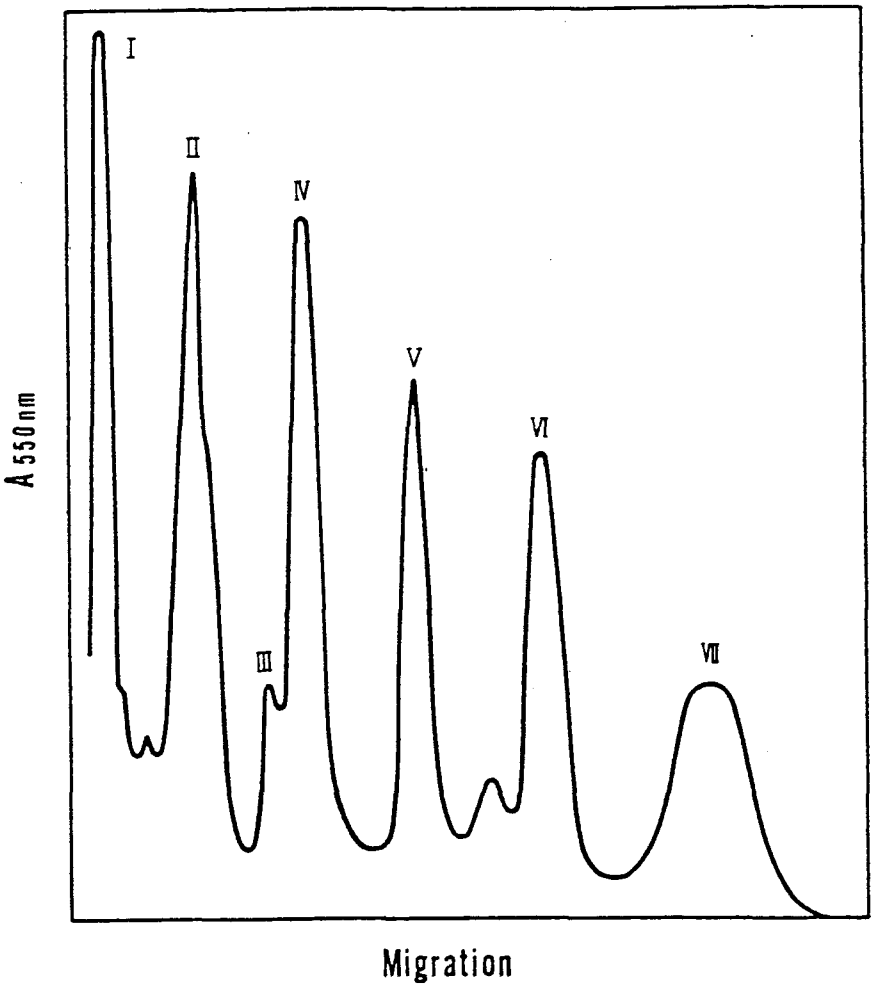

Fig. II-1. Densitometric tracing of SDS polyacrylamide gel electophoresis profile of purified cytochrome oxidase

counter as described in CHAPTER I. The distance between the sample and the counter was calibrated to be 306.4 mm from the powder diffraction of sodium myristate. The measurement times of the scattering intensities were 15 min for the oxidase and the mixture with cytochrome *c* solutions, and 60 min for cytochrome c solution, which could give a meaningful scattering intensity distribution in the range of scattering angles, 2θ = 4.0 - 76.7 mrad, corresponding to Bragg spacings of 400 - 20 Å. For the background intensity correction, the scattering intensities from the same buffer solution as the protein was solubilized in were also recorded under the identical experimental conditions with the protein solutions. All the small-angle X-ray scattering intensity measurements were performed at 14 ± 1 °C. The measured scattering intensities were processed in accordance with the procedure described in CHAPTER I, in which the reliability factors, R_{sym} were good (Table II-2).

Measurement of sedimentation velocity

The sedimentation velocity measurement was carried out at 20.0 °C on a Beckman Spinco E ultracentrifuge in conventional way for using double sector cell. Schlieren optics was employed to record the position of the boundary gradient curves as the function of time. The rotor speed was 8 000 rpm.

3. Results

Cytochrome oxidase-cytochrome c mixture solutions in various concentrations of Tris-HCl buffer, pH 8.0, containing 1% cholate

The radii of gyration, R_g of cytochrome oxidase and cytochrome *c* derived from Guinier plots were 64.0 Å and 19.0 Å,

Table II-2. Reliability factors, R_{sym} of the small-angle X-ray scattering intensities from cytochrome oxidase-cytochrome *c* mixture, cytochrome oxidase and cytochrome *c* solutions

Conc. of buffer* (mM)	R^1_{sym}	R^2_{sym}	R^3_{sym}
4.5	0.076	0.102	0.112
9.0	0.069	0.071	0.105
13.0	0.074	0.096	0.117
17.5	0.066	0.091	0.109
25.0	0.059	0.081	0.101
35.4	0.068	0.081	0.094
44.2	0.070	0.059	0.096
52.0	0.058	0.083	0.110
68.7	0.065	0.071	0.090
84.2	0.061	0.068	0.084

* Tris-HCl buffer, pH 8.0, containing 1% cholate

[1] R_{sym} of cytochrome oxidase-cytochrome *c* mixture

[2] R_{sym} of cytochrome oxidase

[3] R_{sym} of cytochrome *c*

respectively. Neither the radius of gyration of the oxidase nor that of cytochrome *c* were dependent on buffer concentrations within an experimental error. However, the Guinier plot of the small-angle X-ray scattering intensities of the mixture solution of the oxidase and cytochrome *c* (1 : 1 mol/mol) at low buffer concentration (4.5 mM) gave the radius of gyration as 66.0 Å, which was gradually decreased as the buffer concentration was increased, and levelled off with R_g = 62.1 Å at the buffer concentration above 50 mM as shown in Fig. II-2. This tendency of the R_g of the mixture solutions strictly indicates the dissociation of cytochrome oxidase-cytochrome *c* complex (1 : 1 mol/mol) into each component, that is, cytochrome oxidase and cytochrome *c*.

In order to characterize the dissociation of the complex in detail, the degree of dissociation of the complex in each buffer concentration was calculated from the small-angle X-ray scattering intensities from the mixture, the complex, the oxidase and cytochrome *c* solutions with the scattering angle, 2θ higher than that used in the calculation of the radius of gyration. It is reasonable to assume that the scattering intensities from the mixture solution in each buffer concentration are expressed as the summation of the scattering intensities from the complex, the oxidase and cytochrome *c*, because the mixture solution is diluted enough to neglect the interparticle interference and the net scattering intensities are independent on buffer concentration. The observed scattering intensities from the mixture solution, $I_{obs}(s)$ is consequentially expressed as

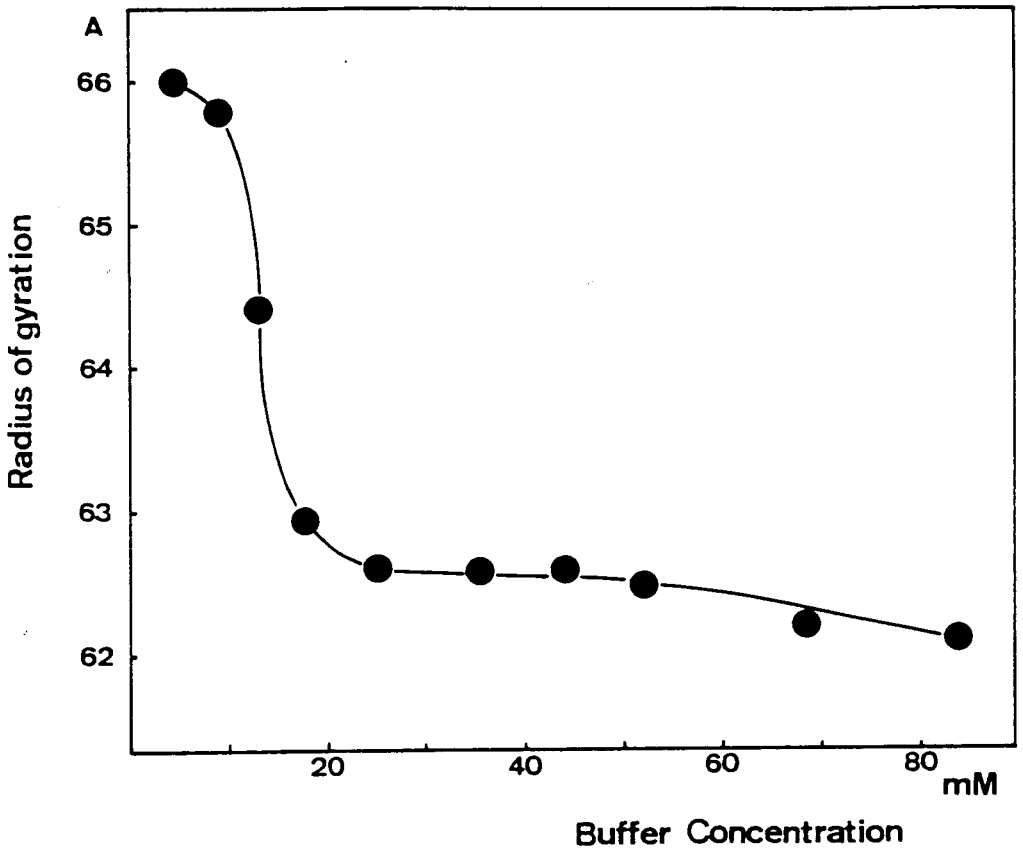

Fig. II-2. Radius of gyration, R_g of cytochrome oxidase-cytochrome *c* mixture in various concentrations of Tris-HCl buffer, pH 8.0, containing 1% cholate

$$I_{obs}(s) = a\, I_{complex}(s) + b\, I_{oxidase}(s) + c\, I_{cyt\text{-}c}(s)$$

where $I_{complex}(s)$, $I_{oxidase}(s)$ and $I_{cyt\text{-}c}(s)$ are the scattering intensities per 1mM of protein per second from the complex, the oxidase and cytochrome *c* solutions. The unknown coefficients of *a*, *b* and *c* are determined by the least-squares method under the condition of $b = c$, because the mixing ratio of the oxidase and cytochrome *c* in the mixture solution is unity. The scattering intensities from the mixture solution in the buffer concentration of 4.5 mM were used as those from the complex solution, $I_{complex}(s)$ on the assumption that all of the oxidase forms the complex with cytochrome *c* in the buffer concentration. From the values of *a* and *b*, the degree of dissociation, α was estimated with the following equation :

$$\alpha = \frac{b}{(a + b)}$$

which is plotted against buffer concentration (Fig. II-3). The figure gave the information about the dissociation of the complex in each buffer concentration more precise than that of the plotting of the radius of gyration, Fig. II-2. It was shown from Fig. II-3 that the dissociation of the complex was increased with the increase of buffer concentration, that is, about half of the complex molecules was dissociated into the oxidase and cytochrome *c* in the buffer concentration of 15 mM and almost all of the complex molecules were levelled off in that of about 45 mM.

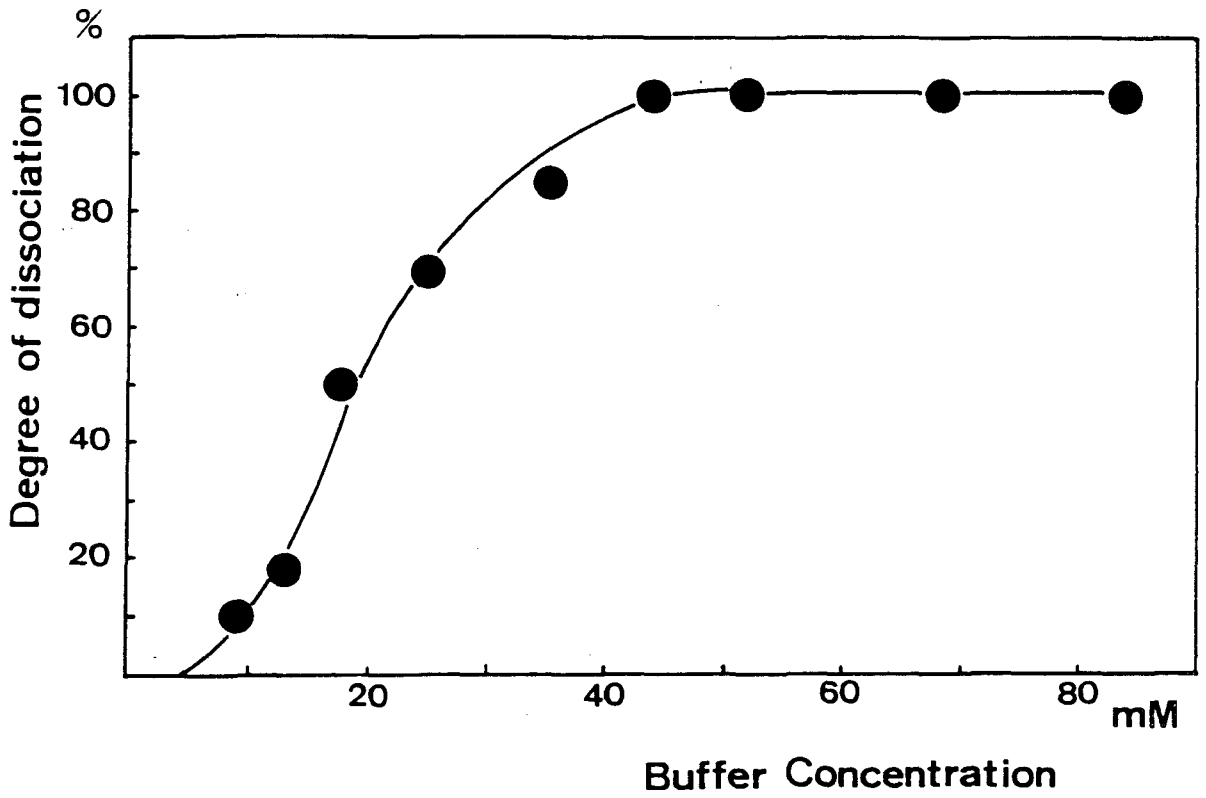

Fig. II-3. Degree of dissociation of cytochrome oxidase-cytochrome *c* complex in various concentrations of Tris-HCl buffer, pH 8.0, containing 1% cholate

Cytochrome oxidase and cytochrome oxidase-cytochrome c complex solutions

Since cytochrome oxidase-cytochrome *c* complex was expected to be formed in low buffer concentration as mentioned above, the small-angle X-ray scattering intensities from cytochrome oxidase-cytochrome *c* mixture solution in the buffer concentration of 4.5 mM were used as those from the complex solution. Cytochrome oxidase solution was that in the buffer concentration of 4.5 mM, because the scattering intensities from the oxidase solutions were independent on buffer concentration.

The radii of gyration, R_g of the complex and the oxidase were determined to be 66.0 Å and 64.0 Å from the Guinier plots of the scattering intensities, respectively. The distance distribution functions, $P(r)$ of the complex and the oxidase are given in Fig. II-4 with that of cytochrome *c*, from which the maximal dimensions, D_{max} were estimated as 250 Å, 210 Å and 40 Å, respectively. The difference distribution function, $D\text{-}P(r)$ (Fig. II-5) was then calculated by the Fourier transformation of ($I_{complex}(s) - I_{oxidase}(s) - I_{cyt\text{-}c}(s)$), where $I_{complex}(s)$, $I_{oxidase}(s)$ and $I_{cyt\text{-}c}(s)$ were defined above. The volumes of the complex and the oxidase were estimated as 9.9×10^5 Å^3 and 8.6×10^5 Å^3 from the equation [A-8] (see appendix), respectively. For the determination of Q in the equation, the integration was carried out numerically up to $s = 0.31$ Å^{-1} ($2\theta = 76.7$ mrad) and the remaining tail end of the scattering intensity curve was integrated analytically according to Porod (18). The molecular weight was then calculated from the equation [A-10]. The partial specific

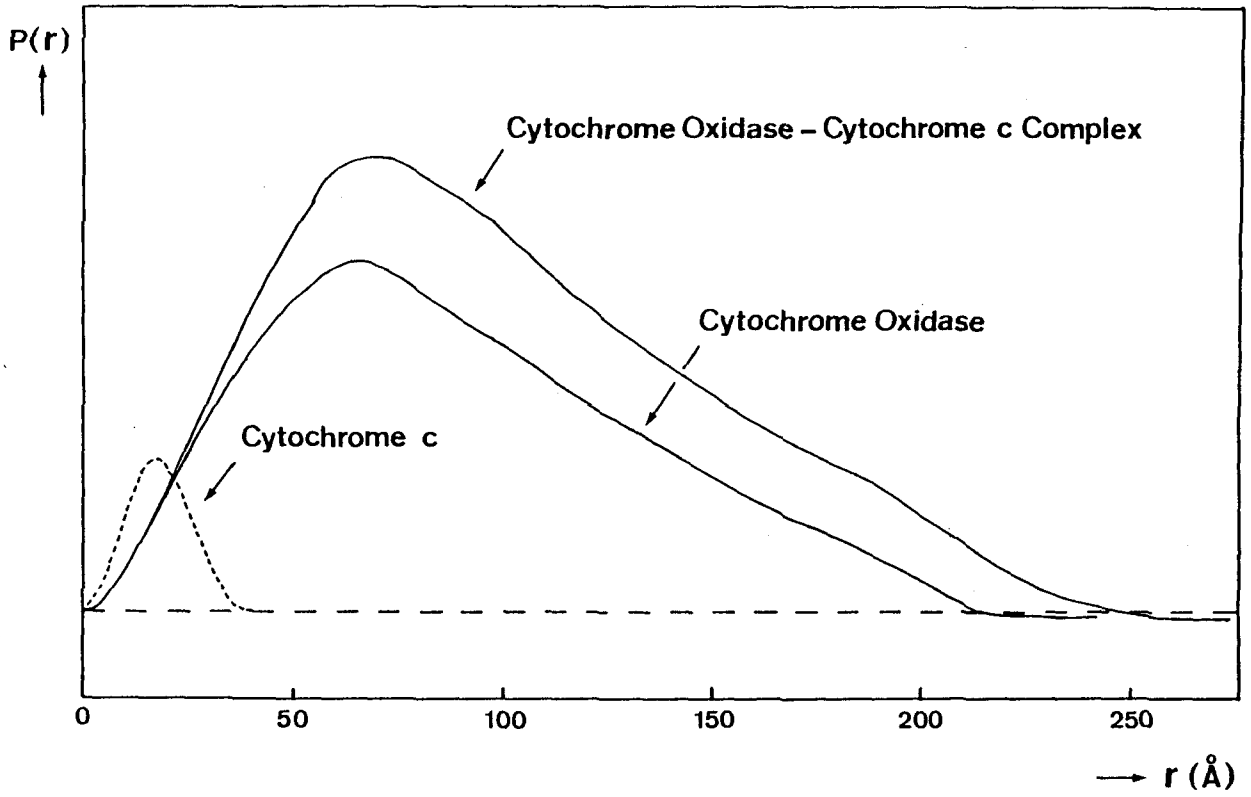

Fig. II-4. Distance distribution functions, $P(r)$ of cytochrome oxidase-cytochrome *c* complex, cytochrome oxidase and cytochrome *c*

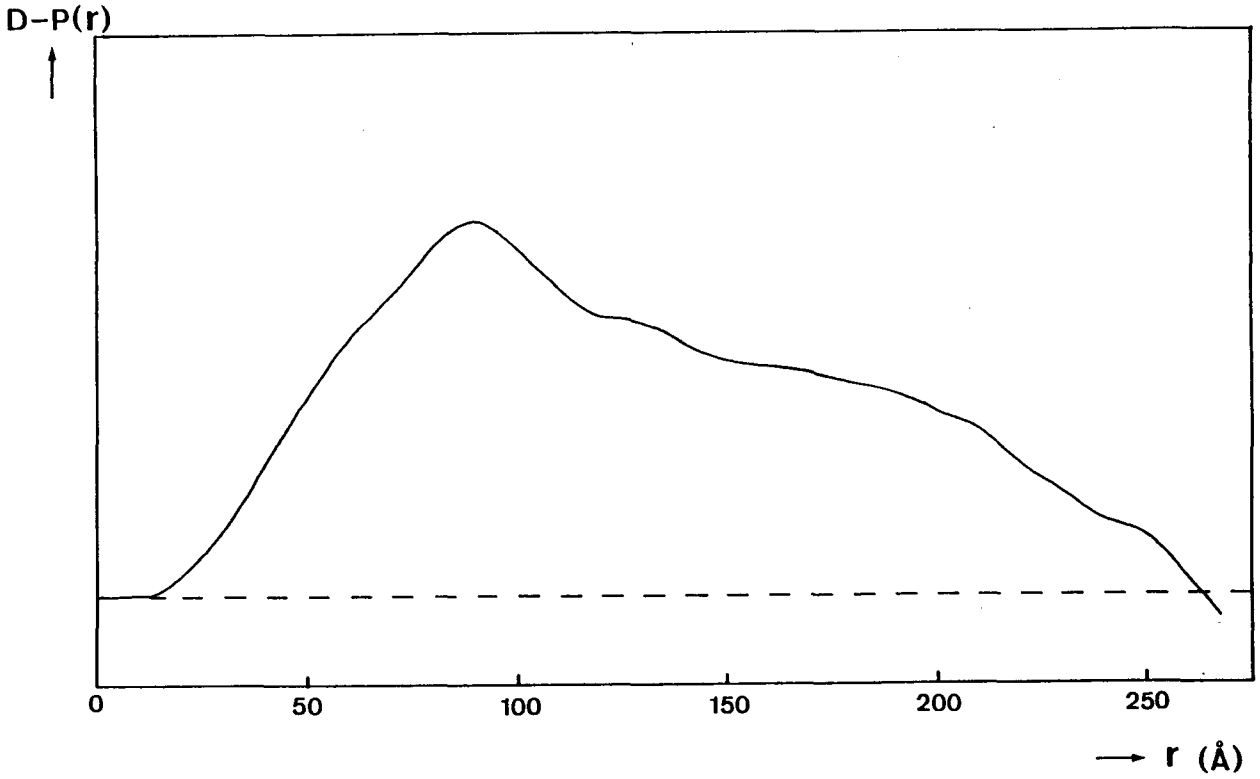

Fig. II-5. Difference distance distribution function, $D\text{-}P(r)$

volume of the oxidase in the equation is calculated to be 0.743 ml/mg (19) from the amino acid composition (20), neglecting the cholate bound to the oxidase, because the amount of cholate bound to the oxidase was expected to be little (19) and the partial specific volume of cholate micelles (0.778 ml/ g (21) in DOC micelles) is comparable with that of the oxidase. The molecular weights of the complex and the oxidase were calculated as 8×10^5 and 7×10^5, respectively.
The sedimentation velocity measurement of the oxidase gave the sedimentation coefficient of $s_{20,w}$ = 17 S. The molecular parameters of the complex and the oxidase are summarized in Table II-3.

Table II-3. Molecular parameters of cytochrome oxidase-cytochrome *c* complex and cytochrome oxidase

Parameter	Complex[1]	Oxidase[2]
Radius of gyration, R_g	66.0 (Å)	64.0 (Å)
Maximal dimension, D_{max}	250 (Å)	210 (Å)
Molecular volume, V	9.9×10^5 (Å^3)	8.6×10^5 (Å^3)
Molecular weight, M_r	8×10^5	7×10^5
Sedimentation coefficient, $s_{20,w}$	-	17 S

[1] cytochrome oxidase-cytochrome *c* complex

[2] cytochrome oxidase

4. Discussion

The change of the radius of gyration of cytochrome oxidase upon the complex formation with cytochrome *c* was successfully detected by small-angle X-ray scattering method as shown in Fig. II-2. The change of the radius of gyration was sharply depended on the buffer concentration. The decrease in the radius of gyration of cytochrome oxidase-cytochrome *c* mixture solution according to the increase of buffer concentration can be interpreted in the following way. Since the radius of gyration of the oxidase is 64.0 Å, the radius of gyration of 66.0 Å means that the oxidase forms the complex with cytochrome *c*, that is, if not, the radius of gyration would be smaller than that of the oxidase due to the contribution of cytochrome *c* to the scattering intensities. The radius of gyration of 62.1 Å, which is 1.9 Å smaller than that of the oxidase, means that the complex is dissociated into the oxidase and cytochrome *c*.

The degree of dissociation was directly determined from the simulation of the scattering intensities from the mixture solution with those from the complex, the oxidase and cytochrome *c* solutions. Fig. II-3 clearly shows that the binding of cytochrome *c* to the oxidase is dependent on buffer concentration. The association constant, K_A of the oxidase and cytochrome *c* could be determined from the degree of dissociation.
Fig. II-6 shows the relationship of K_A with ionic strength of solvent, I, which was estimated from the concentrations of buffer and cholate used as a detergent. The log K_A was decreased almost linearly with the increase of $I^{1/2}$.
The relationship of log K_A with $I^{1/2}$ strictly indicates from

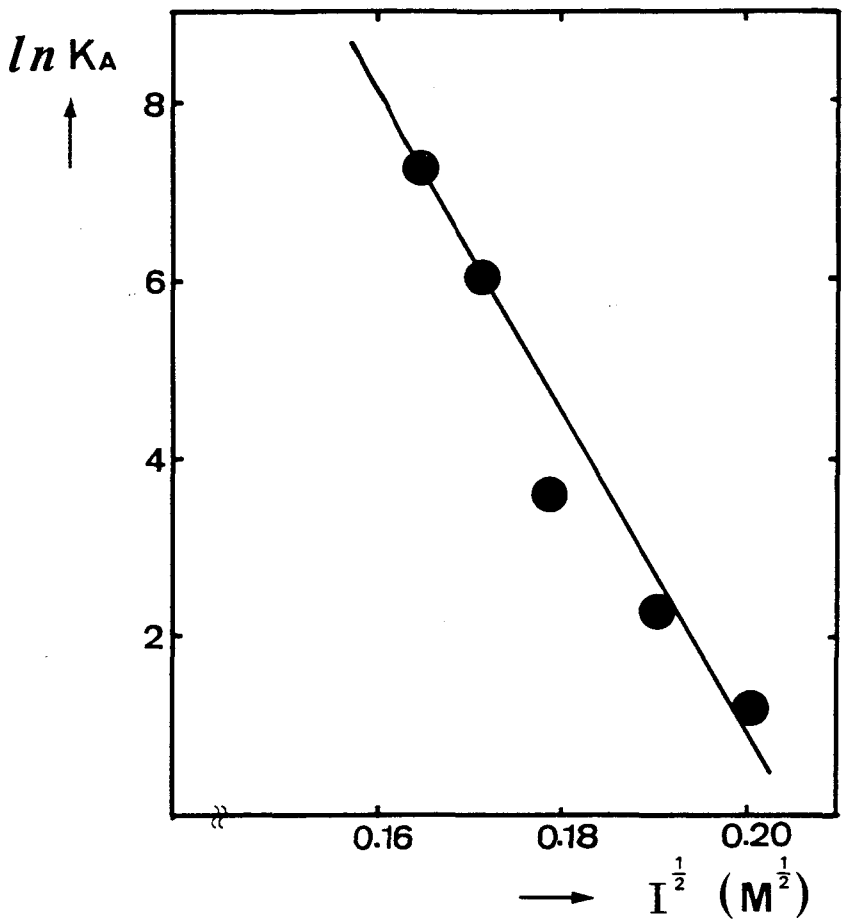

Fig. II-6. Association constant, K_A of cytochrome oxidase and cytochrome *c* in various ionic strengths, *I*

the theories established by Debye, Hückel and Brønsted that the ionic interactions mainly cause the binding of cytochrome *c* to the oxidase. The interactions expect that cytochrome *c* binds with the oxidase on its hydrophilic surfaces.

The radii of gyration of the complex and the oxidase were 66.0 Å and 64.0 Å, respectively. The distance distribution functions of the complex and the oxidase gave the maximal dimensions of 250 Å and 210 Å, respectively, and showed asymmetrical profiles in comparison with symmetrical one of approximately spherical cytochrome *c*. These asymmetrical profiles fulfil that the shapes of the complex and the oxidase are one of those for elongated particles deviated from a sphere (22). Assuming the shapes of the complex and the oxidase as an ellipsoid of revolution with uniform electron density, the ratio of the principal axes, w were estimated to be 2.2 and 1.6 for the complex and the oxidase, respectively, from the equation of $R_g = a\ [(\ 2 + w^2)/5]^{1/2}$ (23), where a is the half length of the principal axis ($a = D_{max}/(2w)$).

The molecular weights of the complex and the oxidase are determined as 8×10^5 and 7×10^5, respectively, which is reasonable in comparison with the sedimentation coefficient of $s_{20,w}$ = 17 S. Since Ozawa *et al.* (24) have reported that the oxidase isolated from beef heart mitochondria has a minimal molecular weight of approx. 130 000, the molecular weights indicate that, in the presence of cholate, the complex and the oxidase exist as a tetramer in solution.

The maximal dimension of the complex was 250 Å, which is 40 Å larger than that of the oxidase. In addition, the

difference distance distribution function, which represents the distribution of pairs different electrons separated by the distance, r between the oxidase and cytochrome c in the complex, gave the distance distribution until r = ~ 260 Å, which is comparable with the maximal dimension of the complex (D_{max} = 250 Å). These results exhibit that cytochrome c binds on the top of the elongated oxidase molecule upon forming the complex with the oxidase.

Recently, Henderson *et al.* (25) have reported from the electron microscopic study on two-dimensional vesicle crystal in mitochondrial inner membrane that cytochrome oxidase has the "Y" shape with maximal dimension of 110 Å and is incorporated in lipid bilayer as shown in Fig. II-7. Summarizing the informations from the small-angle X-ray scattering study and that from the electron microscopic study, the models for the complex and the oxidase in solution were set up (Fig. II-8).

However, as capaldi *et al.* (19) has reported that, in the presence of nonionic detergents such as Triton X-100 and Tween series, the oxidase exists as a dimer, the detergent used greatly influences the state of the oxidase in solution. From this point of view, the small-angle X-ray scattering studies on the oxidase in the presence of the nonionic detergents would have to be done in correlation with the enzymatic activities.

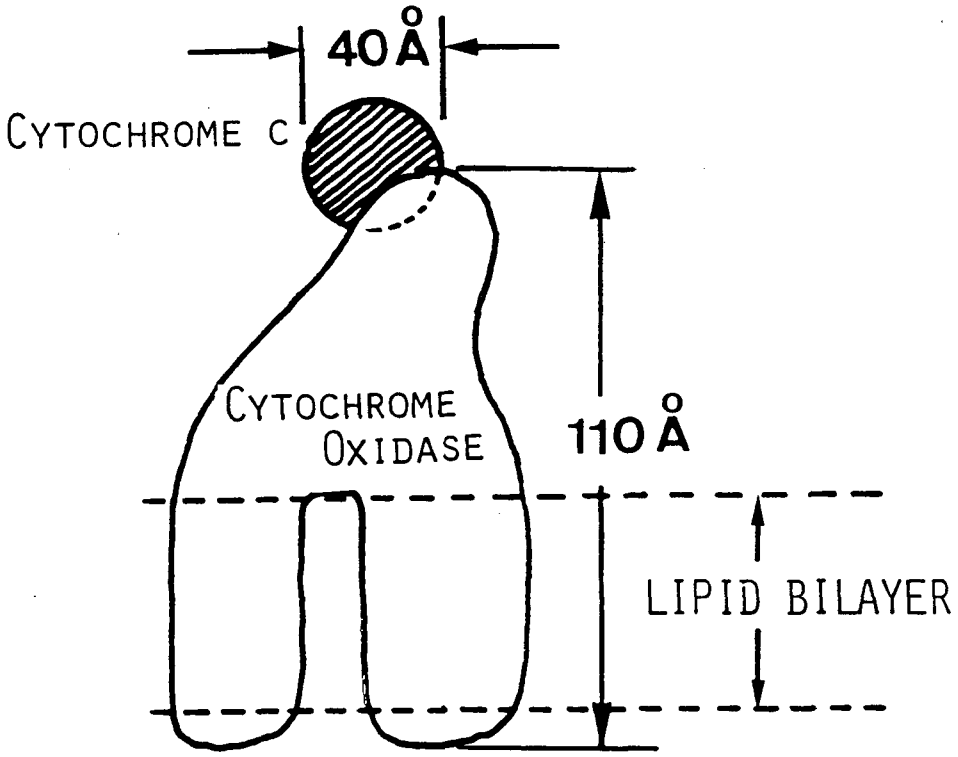

Fig. II-7. Cytochrome oxidase incorporated in lipid bilayer (25)

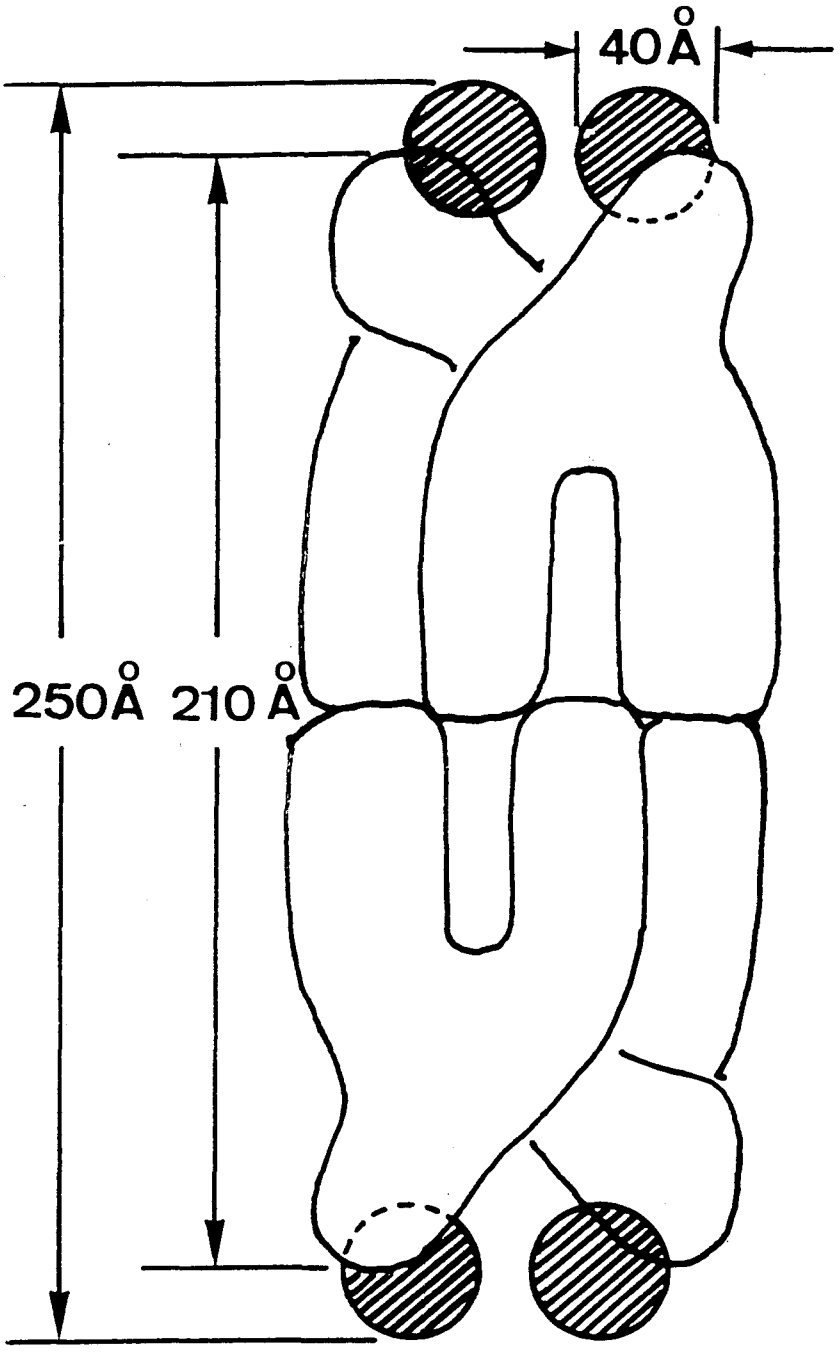

Fig. II-8. Models of cytochrome oxidase-cytochrome *c* complex and cytochrome oxidase in solution

CHAPTER III

Structural Study on Cytochrome Oxidase Isolated from *Nitrobacter agilis*

1. Introduction

Cytochrome aa_3-type oxidase, *i.e.* cytochrome oxidase (EC 1.9.3.1) is widely distributed not only among eukaryotes but also among many prokaryotes (26-28). Although the oxidase of eukaryote has been extensively studied by many investigators (28,29), their structural and functional relationship is still obscure. The molecular level studies of bacterial oxidase of the cytochrome aa_3-type started a few years ago (30-32), and little has been known about its structural aspect, though the oxidase has been purified to some extent from some kinds of bacteria. It has been confirmed by a few researchers, although most of the oxidases isolated from different bacteria resemble the eukaryotic oxidases in some spectral properties, their subunit composition is very different from that of the latter oxidases (33,34). In most of the bacterial oxidases studied so far, the molecule is composed of two kinds of subunits, unlike the eukaryotic oxidases which contain 6-7 kinds of subunits (35).

Recently, Yamanaka *et al.* have reported that the oxidase isolated from *Nitrobacter agilis* has two kinds of subunits of 40 000 and 27 000 daltons with two heme *a* groups and two copper atoms (36). However, it is not confirmed how many copies of the subunit are assembled in the active form.

In this chapter, I have investigated the structure of the oxidase isolated from *Nitrobacter agilis* in solution in order to characterize its active form, and studied the denaturation process of the oxidase by SDS in connection with the active form by small-angle X-ray scattering method in combination with analytical ultracentrifugation.

2. Experimental

Heme *a* concentration was determined from the absorbance at α peak after reduction with $Na_2S_2O_4$ using millimolar extinction coefficient of 20.7 (36). Protein concentration was determined by the method of Lowry *et al.* (37).

Isolation and purification of cytochrome oxidase

Cytochrome oxidase was isolated by Yamanaka's group from *Nitrobacter agilis* (ATCC 14123) cultivated with the medium described by Aleem and Alexander (38). Details of the large scale cultivation is described in Ref. 36. The isolation and purification procedure of the oxidase is presented in Table III-1. The specific heme *a* contents of the purified oxidases were both 20.0 nmol/mg in the presence of Triton X-100 and Tween 20. The densitometric tracing of SDS polyacrylamide gel electrophoresis profile of the purified oxidase is shown in Fig. III-1.

Preparation of samples for small-angle X-ray scattering studies and analytical ultracentrifugations

The purified cytochrome oxidase was dialyzed against 10 mM Tris-HCl buffer, pH 8.0, containing 1% Triton X-100 or 1% Tween 20. The oxidase solutions in the absence of SDS were prepared

Table III-1. Isolation and purification procedure of cytochrome oxidase

---

Whole cells (about 25 g)

↓ Suspended in 100 ml of deionized water

↓ Treated with a sonic oscillator for 20 min

↓ Treated twice with a French pressure cell at 400 kg/cm^2

↓ Centrifuged at 3 000 x g for 10 min

sup

↓ Centrifuged at 60 000 x g for 60 min

ppt

↓ Suspended in 75 ml of 0.1 M Tris-HCl buffer, pH 8.0, containing 1% Triton X-100 and 0.1 M KCl

↓ Treated with the sonic oscillator for 20 min

↓ Centrifuged at 60 000 x g for 60 min

sup

↓ Dialyzed overnight against 20 mM Tris-HCl buffer, pH 8.0, containing 1% Triton X-100.

↓ Charged onto DEAE-cellulose column (4 x 20 cm) equilibrated with 20 mM Tris-HCl buffer, pH 8.0, containing 1% Triton X-100.

↓ Washed with 100 ml of the equilibrium buffer

↓ Eluted with 20 mM Tris-HCl buffer, pH 8.0, containing 1% Triton X-100 and 0.1 M NaCl

↓ Dialyzed against 20 mM Tris-HCl buffer, pH 8.0, containing 1% Triton X-100

↓ Charged onto DEAE-cellulose column (2 x 30 cm) equilibrated with 20 mM Tris-HCl buffer, pH 8.0, containing 1% Triton X-100

↓ Eluted with a linear gradient (0 - 0.12 M) of NaCl in total volume of 400 ml of 20 mM Tris-HCl buffer, pH 8.0, containing 1% Triton X-100

Table III-1. (continued)

↓ Concentrated by adsorption on and elution from an appropriate DEAE-cellulose column

↓ Charged onto Sephadex G-150 column equilibrated with 0.1 M Tris-HCl buffer, pH 8.0, containing 1% Tritox X-100 or Tween 20

↓ Eluted with 0.1 M Tris-HCl buffer, pH 8.0, containing 1% Triton X-100 or 1% Tween 20

↓

Purified cytochrome oxidase

---

sup : supernatant

ppt : precipitate

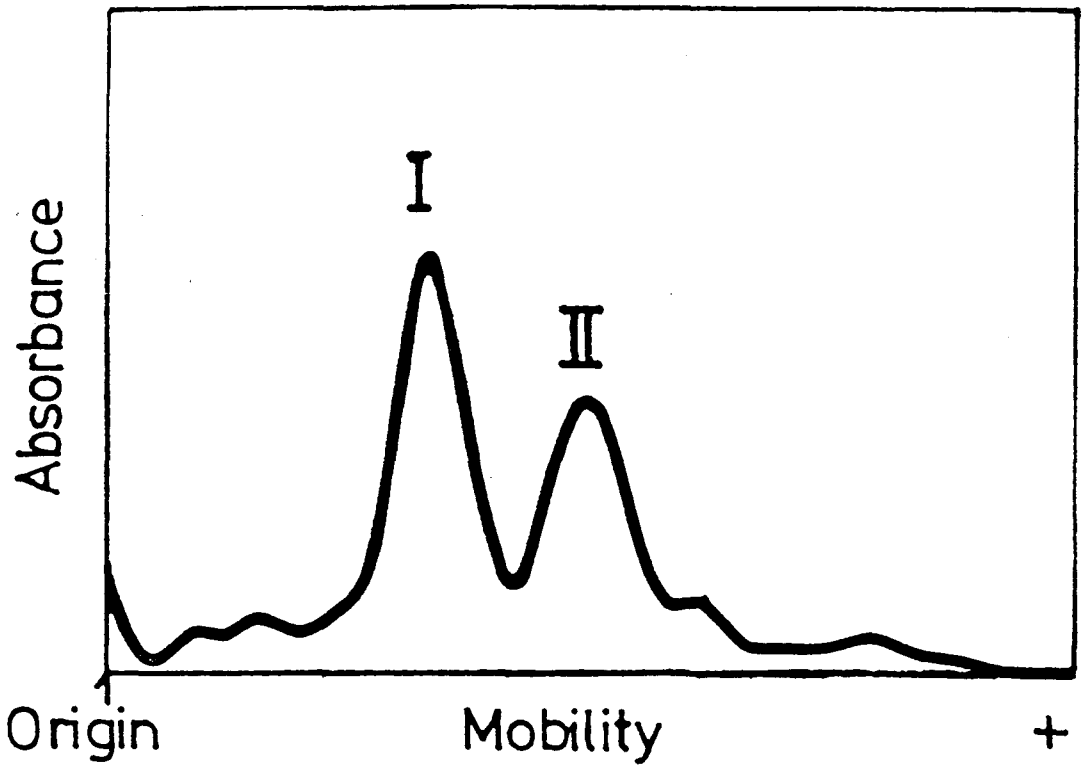

Fig. III-1. Densitometric tracing of SDS polyacrylamide gel electrophoresis of purified cytochrome oxidase

with the same buffer as used in the dialysis. The oxidase solutions in the presence of SDS were also prepared with the same buffer as used in the dialysis by the addition of SDS.

Measurements of small-angle X-ray scattering intensities

The measurements of small-angle X-ray scattering intensities were done on the system equipped with a position-sensitive proportional counter as described in CHAPTER I.

The distance between the sample and the counter was calibrated to be 313.0 mm from the powder diffraction of sodium myristate. The measurement times of the scattering intensities were all 30 min, which could give a meaningful scattering intensity distribution in the range of scattering angles, 2θ = 4.0 - 76.7 mrad, corresponding to Bragg spacings of 400 - 20 Å.

For the background intensity correction, the scattering intensities from the same buffer solution as the oxidase was solubilized in were also recorded under the identical experimental conditions with the oxidase solutions. All the small-angle X-ray scattering intensity measurements were carried out at 14 ± 1 °C. The measured scattering intensities were processed in accordance with the procedure described in CHAPTER I, in which the reliability factors, R_{sym} were good (Table III-2).

Measurements by analytical ultracentrifugation

Both of the sedimentation velocity and the sedimentation equilibrium measurements were carried out on a Beckman Spinco E ultracentrifuge equipped with a photoelectric scanning system.

The sedimentation velocity was measured at 20.0 °C in the conventional way by using a standard double sector cell. The rotor speed was 52 000 rpm with use of schlieren optics to

record the position of the boundary gradient curves as the function of time.

For the sedimentation equilibrium measurements, the double sector cell with a 12-mm filled Epon centerpiece was used. The height of the solution column was adjusted to be 2.5 mm. The rotor speeds and the temperatures were all 8 000 rpm and 3.0 °C, respectively.

Table III-2. Reliability factors, R_{sym} of the small-angle X-ray scattering intensities from cytochrome oxidase solutions

Conc. of oxidase (mg/ml)	Conc. of SDS (%)	R_{sym}
4.0	0.0	0.0805
6.0	0.0	0.0779
10.0	0.0	0.0658
10.0	0.5	0.0654
10.0	1.0	0.0674
10.0	2.0	0.0675
10.0	3.0	0.0852
10.0	4.0	0.0794

3. Results

Cytochrome oxidase sulutions in the absence of SDS

The homogeneity of cytochrome oxidase in solution was ascertained by the sedimentation velocity measurement. The observed single, sharp and symmetrical schlieren profile (Fig. III-2 (e)) gave the sedimentation coefficient of $s_{20,w}$ = 4.7 S and indicated that the oxidase solution consisted of a homogeneous component and no aggregation was perceived.

The small-angle X-ray scattering intensity measurements of the oxidase solutions were performed on the oxidase concentrations of 10.0 mg/ml, 6.0 mg/ml and 4.0 mg/ml in 10 mM Tris-HCl buffer, pH 8.0, containing 1% Triton X-100. The Guinier plots (Fig. III-3) of the scattering intensities from the three kinds of oxidase solutions with different concentrations gave equal values of the radius gyration, which showed no concentration effect (interparticle interference effect) on the observed scattering intensities. Since the Triton X-100 forms bulky complex micelles with the oxidase above CMC, the contribution of the bound Triton X-100 to the scattering intensities can not be ignored, unlike that of the cholate, which forms small and compact complex micelles with the oxidase, as described in CHAPTER I, the molecular parameters derived from the small-angle X-ray scattering method are not those of the oxidase moiety but of the oxidase-Triton X-100 complex.

The radius of gyration, R_g of the oxidase-Triton X-100 complex was determined as 37.1 Å from the Guinier plot of the scattering intensities. The distance distribution function, $P(r)$ (Fig. III-4) gave the maximal dimension, D_{max} of the

c
b
a

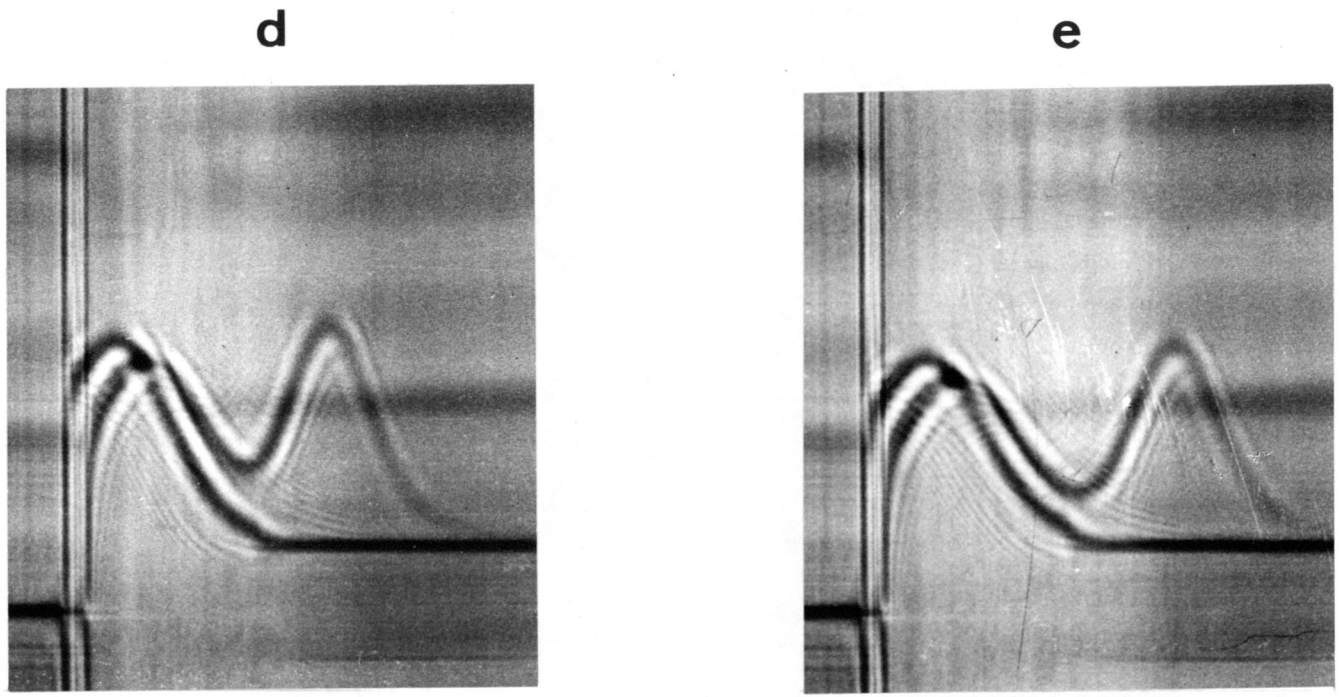

Fig. III-2. Schlieren profiles of cytochrome oxidase-Triton X-100 complex. Sedimentation from left to right. Photographs were taken at (a) 14 min, (b) 24 min, (c) 34 min, (d) 44 min and (e) 54 min after a rotor speed of 52 000 rpm. The protein concentration was 4.0 mg/ml in 10 mM Tris-HCl buffer, pH 8.0, containing 1% Triton X-100.

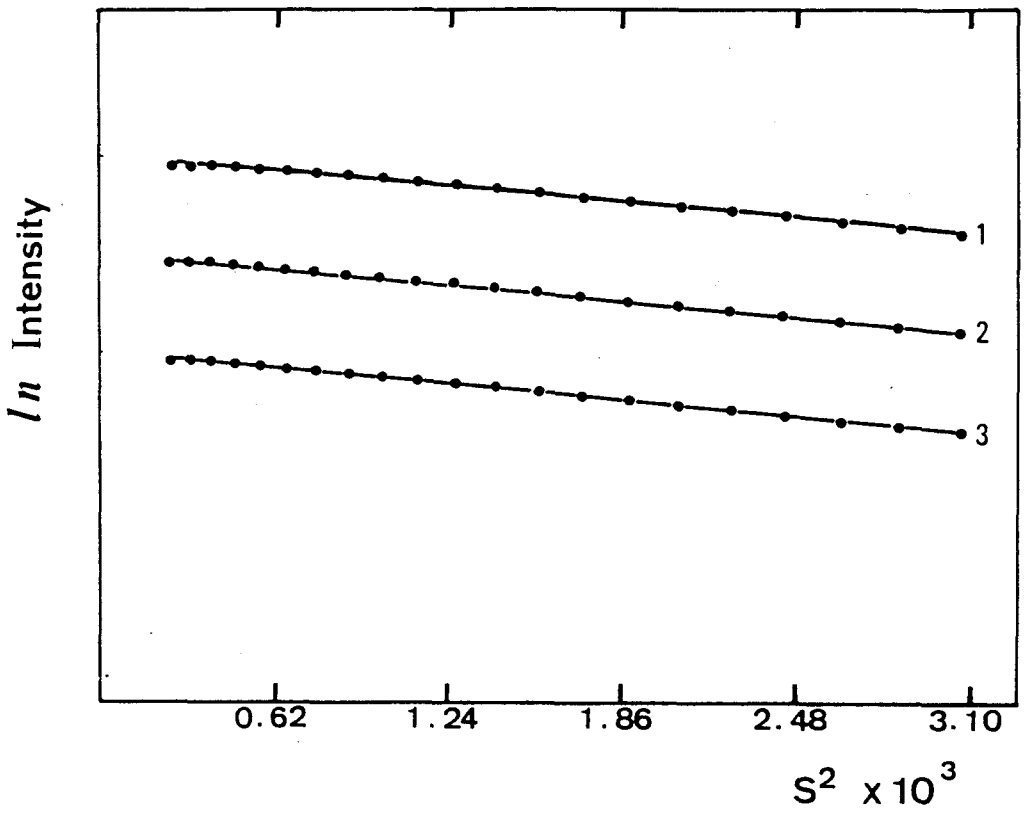

Fig. III-3. Guinier plots of small-angle X-ray scattering intensities from cytochrome oxidase solutions. The oxidase concentrations of the solutions are 1) 10.0 mg/ml, 2) 6.0 mg/ml and 3) 4.0 mg/ml. The intensity is in arbitrary units.

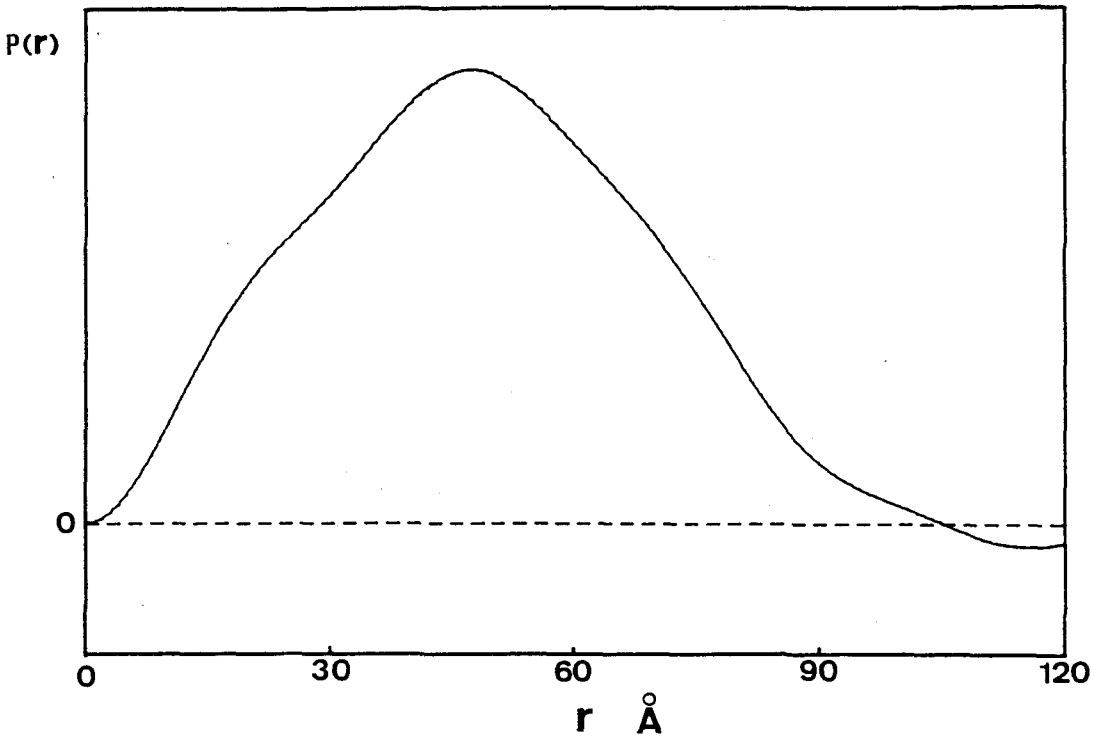

Fig. III-4. Distance distribution function, $P(r)$ of cytochrome oxidase-Triton X-100 complex

complex as 105 Å. Assuming the shape of the complex as an ellipsoid of revolution with uniform electron density, the ratio of the principal axes, w was estimated to be 1.4 from the equation of $R_g = a\ [(\ 2 + w^2)/5]^{1/2}$ (23), where a is half length of the principal axis ($a = D_{max}/(2w)$).

The molecular weight of the oxidase was estimated by using the following equation, which is the modified one of the equation [A-10] for the amount of Triton X-100 bound to the oxidase.

$$M_{od} = \frac{(\ N_A\ V/\bar{v}_c\ )}{(\ x + 1\ )}$$

where N_A is the Avogadro's number, V the volume of the oxidase-Triton X-100 complex, $\bar{v}_c$ the partial specific volume of the complex, x the bound Triton X-100 per the oxidase (g/g) and M_{od} the molecular weight of the oxidase. The value of x was estimated as 0.58 by the method of Capaldi *et al.* (19). $\bar{v}_c$ is closely approximated by (39)

$$\bar{v}_c = \frac{x\ \bar{v}_{tx} + \bar{v}_{od}}{x + 1}$$

where $\bar{v}_{tx}$ is the partial specific volume of Triton X-100 micelles ($\bar{v}_{tx}$ = 0.908 ml/ g (21)) and $\bar{v}_{od}$ that of the oxidase ($\bar{v}_{od}$ = 0.744 ml/ g), which was calculated from the amino acid composition (20) of the oxidase reported by Yamanaka *et al.*(36). The volume, V of the complex was estimated to be 1.6 x 10^5 Å^3 from the equation [A-8]. For the determination of Q in the equation, the integration was carried out numerically up to

s = 0.31 Å^{-1} (2θ = 76.7 mrad) and remaining tail end of the scattering intensity curve was integrated analytically according to Porod (18). From these values, the molecular weight of the oxidase was determined to be 75 000.

The molecular weight of the oxidase was also determined from the results of the sedimentation equilibrium. The measurements of the sedimentation equilibrium were done in the oxidase solutions in the presence of Triton X-100 and Tween 20 in order to investigate the influence of a detergent on molecular weight determination. The log c vs r^2 plots are linear throughout the cell in both the detergents as shown in Fig. III-5, which also means the monodispersion of the oxidase-Triton X-100 or -Tween 20 complex. From the slopes of the plots, the buoyant densities were calculated to be 23 000 and 26 000 for the oxidase-Triton X-100 and -Tween 20 complexes, respectively. The molecular weight of the oxidase, M_{od} and the buoyant density are related by the following equation (21,39)

$$\text{Buoyant density} = M_{od} [1 - \bar{v}_{od} \rho + x(1 - \bar{v}_{d} \rho)] \quad \text{--[III-1]}$$

where ρ is the density of the solvent (ρ = 1.003 and 1.003 mg/ml for 10 mM Tris-HCl buffers, pH 8.0, containing 1% Triton X-100 and containing 1% Tween 20, respectively), $\bar{v}_d$ the partial specific volume of the detergent used, and $\bar{v}_{od}$ and x defined above. The buoyant density with Triton X-100 of 23 000 gave the molecular weight of 73 000. Although the buoyant density with Tween 20 was calculated to be 26 000,

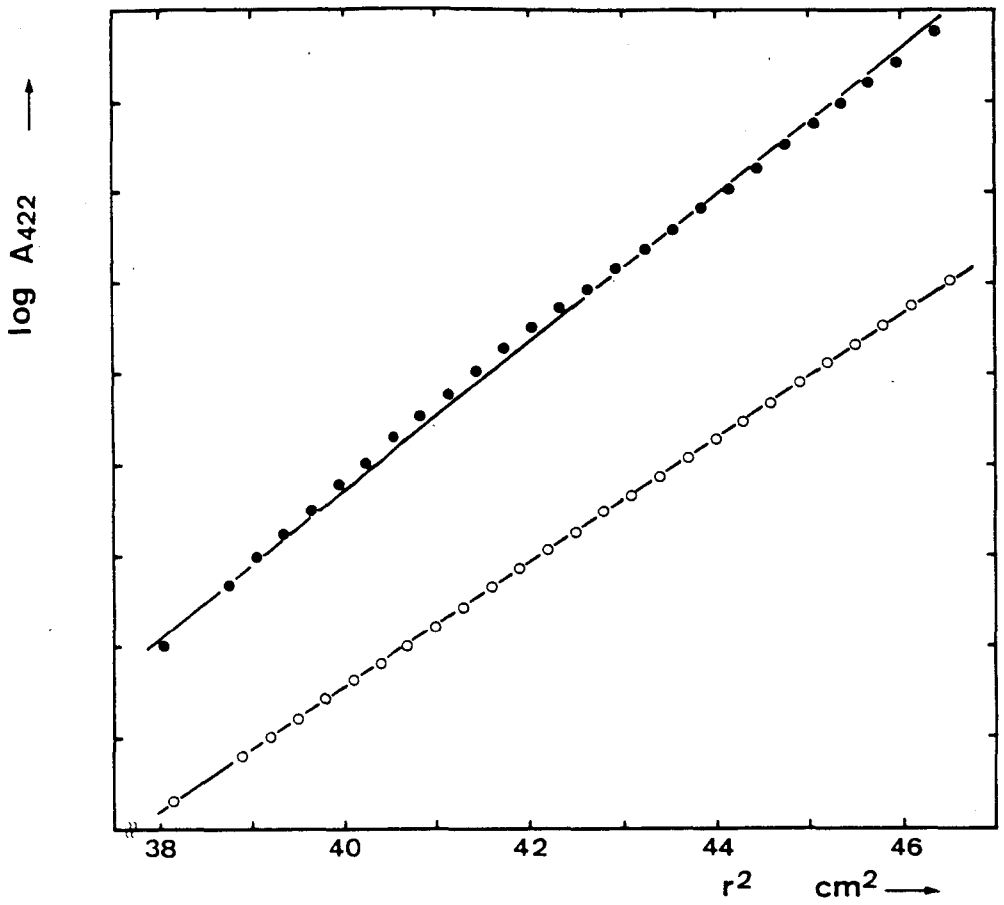

Fig. III-5. Sedimentation equilibriums of cytochrome oxidase-Triton X-100 (—○—) and cytochrome oxidase-Tween 20 (—●—) complexes. The oxidase concentrations are 0.16 mg/ml for both complex solutions.

the molecular weight was not determined, because it was difficult to estimate the value of x due to the lack of quantitative assay for Tween 20. However, assuming that $x = 0$, the molecular weight of the oxidase, M_{od} could be determined to be 102 000 from the equation [III-1]. The molecular parameters and the molecular weights determined from the small-angle X-ray scattering method and the analytical ultracentrifugation are summarized in Table III-3 and Table III-4, respectively.

Table III-3. Molecular parameters of cytochrome oxidase-Triton X-100 complex

Radius of gyration, R_g	37.5 (Å)
Maximal dimension, D_{max}	105 (Å)
r_{max}*	48 (Å)
Molecular volume, V	1.6×10^5 (Å^3)
Sedimentation coefficient, $s_{20,w}$	4.7 S

* r where $P(r)$ peaks

Table III-4. Molecular weight estimations of cytochrome oxidase

Method	in Triton X-100	in Tween 20
X-ray study	75 000	-
Sedimentation equilibrium study	73 000	102 000*
SDS polyacrylamide gel electrophoresis study**	69 000	-
Ferguson plot**	84 000	-

* Not corrected for bound Tween 20

** Yamanaka *et al.* (36)

Cytochrome oxidase solutions in the presence of SDS

The small-angle X-ray scattering intensity measurements of cytochrome oxidase solutions were performed with the SDS concentrations of 0.5%, 1.0%, 2.0%, 3.0% and 4.0% in 10 mM Tris-HCl buffer, pH 8.0, containing 1% Triton X-100. The concentrations of the oxidase were all kept to be 10.0 mg/ml. The scattering intensity curves of the oxidase solutions at each SDS concentration are presented in Fig. III-6, which indicated that the interparticle interference effects (40) were observed on the inner parts of the intensity curves

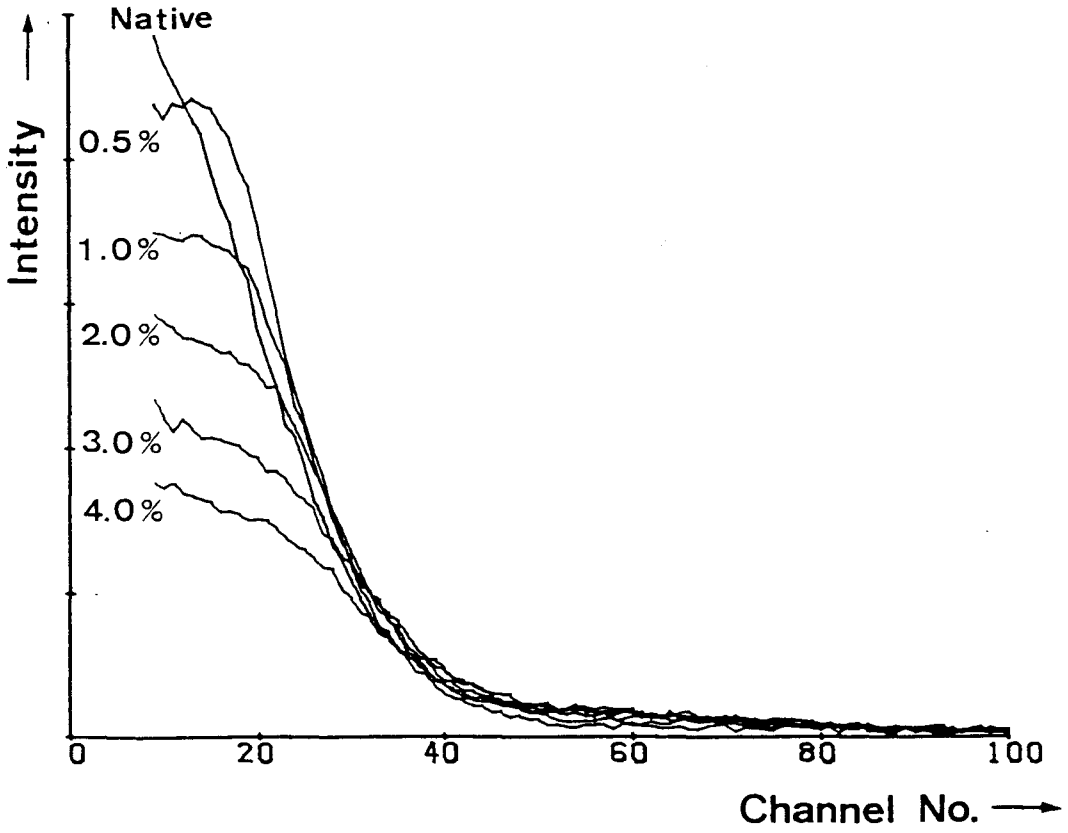

Fig. III-6. Small-angle X-ray scattering intensity curves of cytochrome oxidase solutions in various SDS concentrations

at the SDS concentrations of 0.5% and 1.0%.

The distance distribution functions, $P(r)$ (Fig. III-7) obtained by the Fourier transformation of the scattering intensity curves were greatly changed as the SDS concentration was increased. At the SDS concentration of 0.5%, although the values of of the D_{max} and r_{max} were decreased, the peak height of the $P(r)$ became higher than that of the $P(r)$ at the SDS concentration of 0.0%. However, at the SDS concentrations of above 1.0%, all the values of the peak height, D_{max} and r_{max} were decreased with the increase of SDS concentration.
The radius of gyration, R_g of the oxidase-Triton X-100 complex was greatly decreased from 37.1 Å to 28.6 Å as the concentration of SDS was increased from 0.0% to 1.0%, and was then slowly reduced with the increase of SDS concentration. The same decreases as the radius of gyration, R_g were observed in the values of D_{max}, r_{max} and $I(0)$ as plotted in Fig. III-8.

4. Discussion

It has been reported from an electrophoresis study of cytochrome oxidase isolated from *Nitrobacter agilis* that the oxidase was made of an assembly of the minimal unit that has two kinds of subunits of 40 000 and 27 000 daltons, two heme *a* groups and two copper atoms (36) : the minimal unit of the oxidase is 69 000 daltons. However, a Ferguson plot of the two subunits of the oxidase gave the molecular weights of 51 000 and 31 000, respectively (36) : the minimal unit of the oxidase is 84 000 daltons.

The small-angle X-ray scattering and the sedimentation

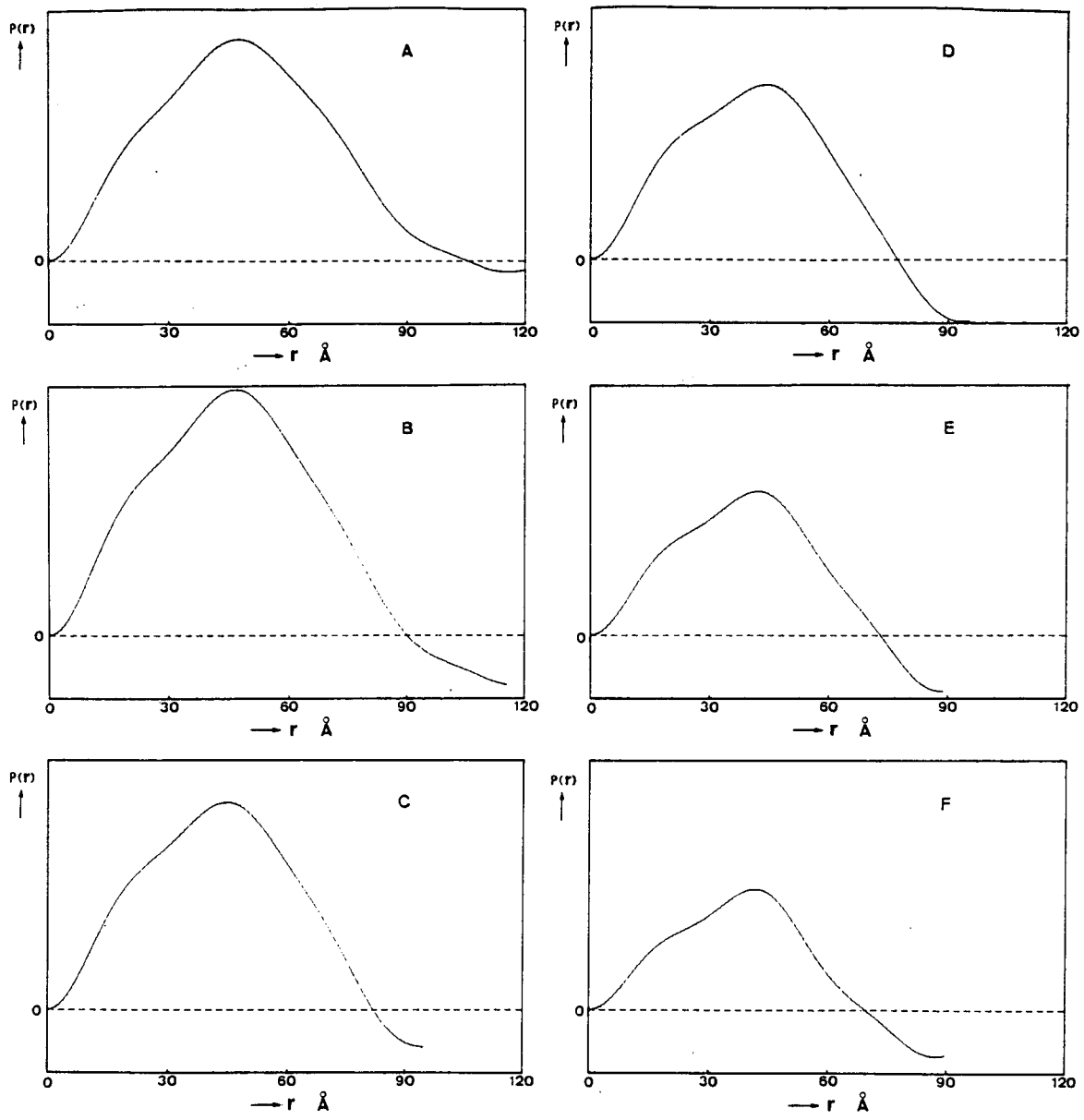

Fig. III-7. Distance distribution functions, $P(r)$ of cytochrome oxidase-Triton X-100 complexes in the presence of various concentrations of SDS, A : 0.0% SDS, B : 0.5% SDS, C : 1.0% SDS, D : 2.0% SDS, E : 3.0% SDS and F : 4.0% SDS

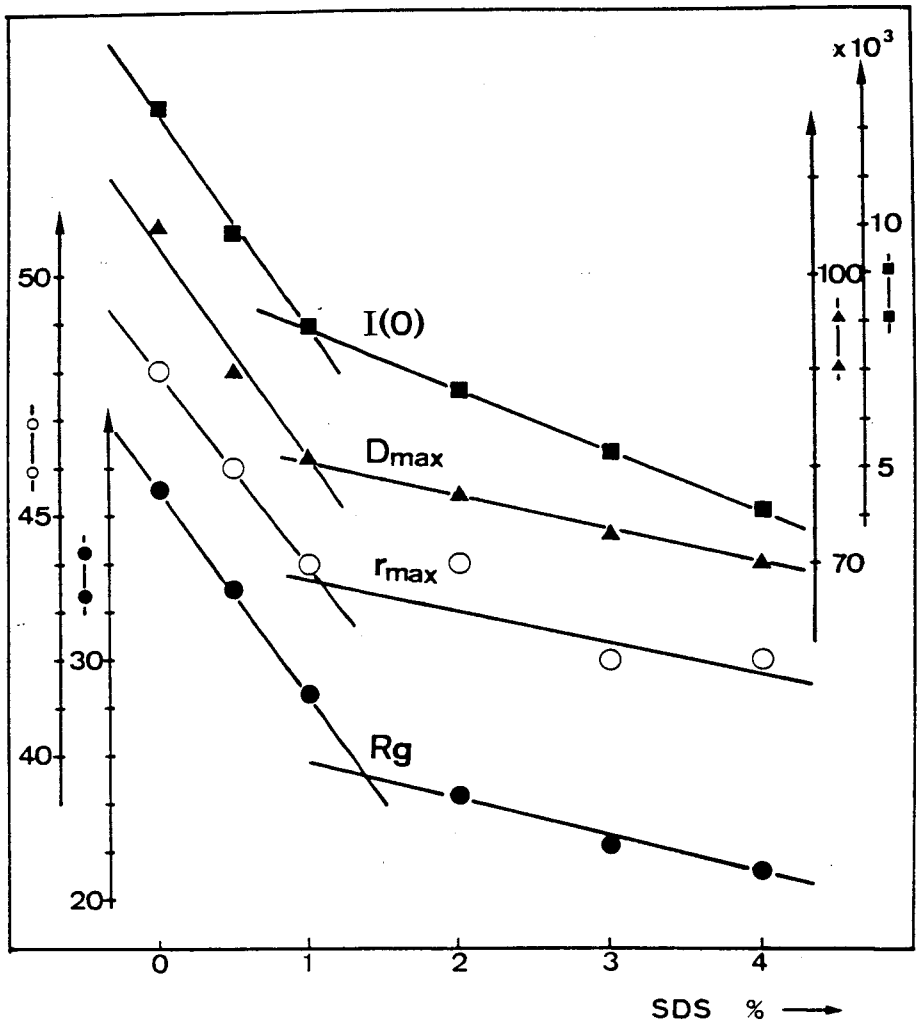

Fig. III-8. Correlations of $I(0)$, D_{max}, r_{max} and R_g with SDS concentration

equilibrium studies showed that, in the presence of Triton X-100, the oxidase has a molecular weight of 75 000 to 73 000, which is reasonable in comparison with the sedimentation coefficient of $s_{20,w}$ = 4.7 S and is comparable with the values obtained from the electrophoresis study. This value means that, in the presence of Triton X-100, the oxidase exists as a monomer containing two subunits, two heme *a* groups and two copper atoms. This result can be compared with the fact that the oxidase isolated from *Paracoccus denitrificans* is monomeric (41). In the presence of Tween 20, the molecular weight of the oxidase could not be determined, because the value of x in the equation [III-1] was not known. However, from the equation [III-1], the value of x could be estimated as 0.78 by utilizing the molecular weight of the oxidase, M_{od} (M_{od} = 73 000) and the partial specific volume of Tween 20 micelles, $\bar{v}_{tn}$ ($\bar{v}_{tn}$ = 0.869 ml/ g (21)). This value of x is not far from that obtained in the presence of Triton X-100.
In this way, the equation [III-1] gives the molecular weight of the oxidase less than 102 000 in the presence of Tween 20, taking account of the value of x, which also implies that, in the presence of Tween 20, the oxidase exists as the monomer.
The specific activities (μmol of cytochrome *c* oxidized / mg protein / min) of the oxidase have been determined to be 260 with *Candida krusei* cytochrome *c* in presence of Triton X-100 and Tween 20 (42), which are very high unlike that of the oxidase from *Paracoccus denitrificans*. The values of the specific activities and the estimations of the molecular weights stated above lead the conclusion that, in the nonionic detergents

such as Triton X-100 and Tween 20, the active form of the oxidase isolated from *Nitrobacter agilis* is composed of two subunits, two heme *a* groups and two copper atoms.

The radius of gyration and the maximal dimension of the oxidase-Triton X-100 complex have been determined to be 37.1 Å and 105 Å, respectively. Assuming the shape of the complex as an ellipsoid of revolution with uniform electron density, the ratio of the principal axes was estimated to be 1.4. In addition, the distance distribution function gave a somewhat asymmetrical profile, the shape of the complex from which is expected to be one of those for elongated particles deviated from a sphere (22). Though it is hard to describe the exact feature of the complex, these results show that the complex may be slightly elongated.

The small-angle X-ray scattering intensity curves of the oxidase solutions in the presence of 0.5% and 1.0% SDS showed interparticle interference effect. The effect attributes to that of the intersubunit interference between the two subunits of the oxidase rather than that of the intermolecular interference between the oxidases, because, in the oxidase solutions in the absence of SDS, the intermolecular interference effect was not perceived. When the SDS was added 1.0% to the solutions, the radius of gyration of the complex was greatly decreased from 37.1 Å to 28.6 Å, and was then slowly reduced with the increase of SDS concentration. The similar decreases as the radius of gyration were observed in D_{max}, r_{max} and $I(0)$, which means that the structure of the complex was drastically changed until 1.0% SDS concentration, followed by the successive

minor structural change above 1.0% SDS concentration. These tendencies on the variation of R_g, D_{max}, r_{max} and $I(0)$ indicate that the denaturation process of the oxidase by SDS consists of two kinds of structural changes. The drastic decreases of R_g and D_{max} may be directly attributed to the breakdown of the oxidase, which is also supported by the fact that the intersubunit interference effect were observed on the oxidase solutions in the presence of 0.5% and 1.0% SDS. From these results, it is suggested that the first step of the denaturation process of the oxidase by SDS is splitting into each subunit and the second is other small structural changes in each subunit such as unfolding of the polypeptide chain in the subunit.

CHAPTER IV

Structural Studies on Taka-Amylase A And *Pseudomonas* Isoamylase

1. Introduction

Taka-amylase A is an α-amylase (EC 3.2.1.1, α-1,4-glucan-4-glucano hydrolase) produced by *Aspergillus oryzae* bred on steamed rice and catalyzes the hydrolysis of the α-1,4-glucosidic linkage in polysaccharides as well as the maltosidic linkages of various α-maltosides such as phenyl-α-maltoside (43,44). This enzyme is composed of a single polypeptide chain of about 460 amino acids and a carbohydrate moiety consisting of 6 mole of mannose and 2 mole of glucosamine linked to the polypeptide chain (45). The amino acid sequence has been already determined by Narita *et al.* (46). The crystal structure analysis has been performed by means of X-ray diffraction at the resolution of 3 Å by Kakudo *et al.* (47). The analysis showed that the enzyme was made of two domains (main domain and C-terminal domain) and has an ellipsoidal shape with approximate dimensions of 35 x 45 x 80 Å with a hollow which corresponds to the active center as shown in Fig. IV-1.

Pseudomonas isoamylase (EC 3.2.1.9, amylopectin 6-glucano hydrolase), which is discovered by Harada *et al.* (48), is an extracellular debranching enzyme isolated from soil bacterium, *Pseudomonas* sp. strain SB 15 and one of enzymes hydrolyzing α-1,6-glucosidic interchain linkages in polysaccharides. Since the enzyme that acts on polysaccharide at its branching

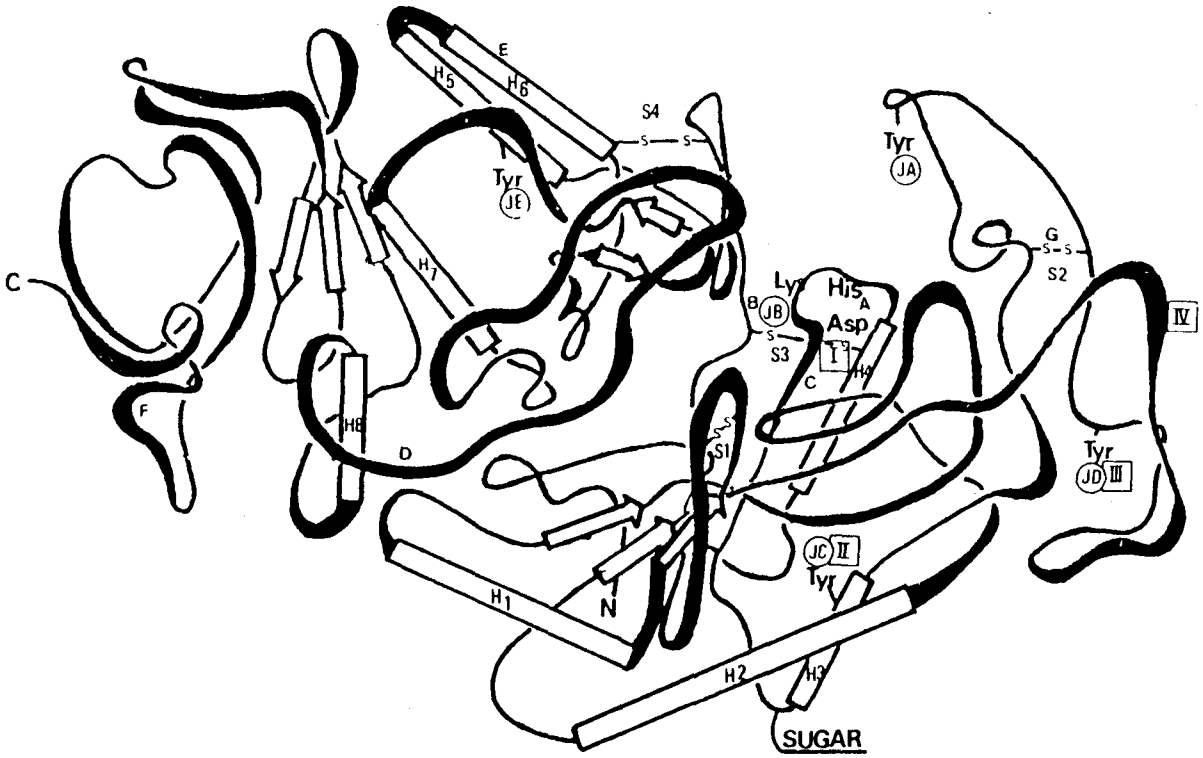

Fig. IV-1. Schematic drawing of Taka-amylase A molecule (47)

point was named isoamylase, Harada *et al.* tentatively named the enzyme produced by *Pseudomonas* sp. strain SB 15 *Pseudomonas* isoamylase. *Pseudomonas* isoamylase hydrolyzes all α-1,6-glucosidic inter-chain linkages in glycogen, amylopectin and their phosphorylase limit dextrins, but the debranching points of β-amylase limit dextrins were not hydrolyzed completely (49). This enzyme is at present widely used in Sugar industory in producing martose in combination with a β-amylase.

In this chapter, small-angle X-ray scattering studies on the sizes and shapes of Taka-amylase A and *Pseudomonas* isoamylase in solution were described. The molecular shape of Taka-amylase A in solution was compared with that in crystal, and the packing of *Pseudomonas* isoamylase in crystal was discussed.

2. Experimental

Isolations and purifications of Taka-amylase A and Pseudomonas isoamylase

Taka-amylase A was isolated from Takadiastase Sankyo, and was purified according to the method of Akabori *et al.* (50), followed by chromatography on a DEAE-cellulose column.

Pseudomonas isoamylase was isolated from the culture fluid *Pseudomonas* sp strain SB 15, and was refractionated with ammonium sulfate, followed by dialysis. The refractionated enzyme was purified by DEAE- and CM-cellulose column chromatographies (49).

Crystallization of Pseudomonas isoamylase

To a 10% solution (in 10 mM acetate buffer, pH 3.5) of

the purified enzyme, an $(NH_4)_2SO_4$ solution was added dropwise in the cold until the solution became turbid. The cloudy solution was kept at 4 °C to grow single crystals with appropriate size for X-ray diffraction study.

Preparation of samples for small-angle X-ray scattering intensity measurements

The purified Taka-amylase A solution was finally dialyzed against 50 mM acetate buffer, pH 4.9, containing 20 mM $Ca(Ac)_2$, and prepared with the same buffer to the protein concentrations ranging from 5.0 - 13.2 mg/ml.

The purified *Pseudomonas* isoamylase was finally dialyzed against 10 mM acetate buffer, pH 3.5, and was prepared with the same buffer to the protein concentrations ranging from 3.6 - 14.6 mg/ml.

The protein concentrations were determined spectrophotometrically using $E^{1\%}_{280nm}$ = 22.1 cm^{-1} and 22.6 cm^{-1}, for Taka-amylase A and *Pseodomonas* isoamylase, respectively.

Measurements of small-angle X-ray scattering intensities

The measurements of small-angle X-ray scattering intensities were carried out on the system equipped with a position-sensitive proportional counter as described in CHAPTER I. The distance between the sample and the counter was calibrated to be 306.4 mm from the powder diffraction of sodium myristate. The measurement times of the scattering intensities were from 60 min to 180 min for Taka-amylase solutions and from 30 min to 90 min for *Pseudomonas* isoamylase solutions, which could give significant scattering intensities in the range of scattering angles, 2θ = 4.0 - 76.7 mrad, corresponding to Bragg

spacings of 400 - 20 Å. For the background intensity correction, the scattering intensities from the same buffer solution as the protein was solubilized in were also recorded under the identical experimental conditions with the protein solutions. All the small-angle X-ray scattering intensity measurements were carried out at 14 ± 1 °C. The measured scattering intensities were processed in accordance with the procedure described in CHAPTER I, in which the reliability factors, R_{sym} were good (Table IV-1 and Table IV-2).

Measurements of X-ray diffraction patterns from Pseudomonas isoamylase crystal

A well-shaped crystal of *Pseudomonas* isoamylase with approximate dimensions of 0.4 x 0.5 x 0.6 mm was sealed in a thin-walled glass capillary with a trace of mother liquor. X-ray diffraction patterns of the *h 0 l* and *0 k l* zones were recorded with a Buerger precession camera (Ni-filtered CuKα radiation, μ = 11.1 ° (approx. 4 Å resolution) and a crystal-to-film distance of 100 mm).

Table IV-1. Reliability factors, R_{sym} of the small-angle X-ray scattering intensities from Taka-amylase A solutions

Conc. of protein (mg/ml)	R_{sym}
5.0	0.124
10.0	0.125
13.2	0.108

Table IV-2. Reliability factors, R_{sym} of the small-angle X-ray scattering intensities from *Pseudomonas* isoamylase solutions

Conc. of protein (mg/ml)	R_{sym}
3.6	0.087
7.3	0.084
10.4	0.084
14.6	0.077

3. Results

Taka-amylase A

The small-angle X-ray scattering intensity measurements were performed on Taka-amylase A solutions of the concentrations of 13.2 mg/ml, 10.0 mg/ml and 5.0 mg/ml in 50 mM acetate buffer, pH 4.9, containing 20 mM $Ca(Ac)_2$. Each of the Guinier plots (Fig. IV-2) of the scattering intensities at different protein concentrations was linear within the limits of errors and parallel with each other, which showed no concentration effect (interparticle interference effect) on the observed scattering intensities.

The radius of gyration, R_g of Taka-amylase A was determined to be 21.0 Å from the slope of the Guinier plot. The distance distribution function, $P(r)$ (Fig. IV-3) gave the maximal dimension, D_{max} of Taka-amylase A as 65 Å. Assuming the shape of Taka-amylase A as an ellipsoid of revolution with uniform electron density, approximate dimensions of the molecule were estimated to be 45 x 45 x 65 Å by the least-squares fitting between observed scattering intensities and theoretical scattering intensities from an ellipsoid of revolution. The volumes of the molecule were determined to be 6.8×10^4 Å^3 and 6.2×10^4 Å^3 from the dimensions of the ellipsoidal molecule and from the small-angle X-ray scattering intensities, using the equation [A-8], respectively. For the determination of Q in the equation, the integration was carried out numerically up to $s = 0.31$ Å^{-1} ($2\theta = 76.7$ mrad) and remaining tail end of the scattering intensity curve was integrated analytically according to Porod (18).

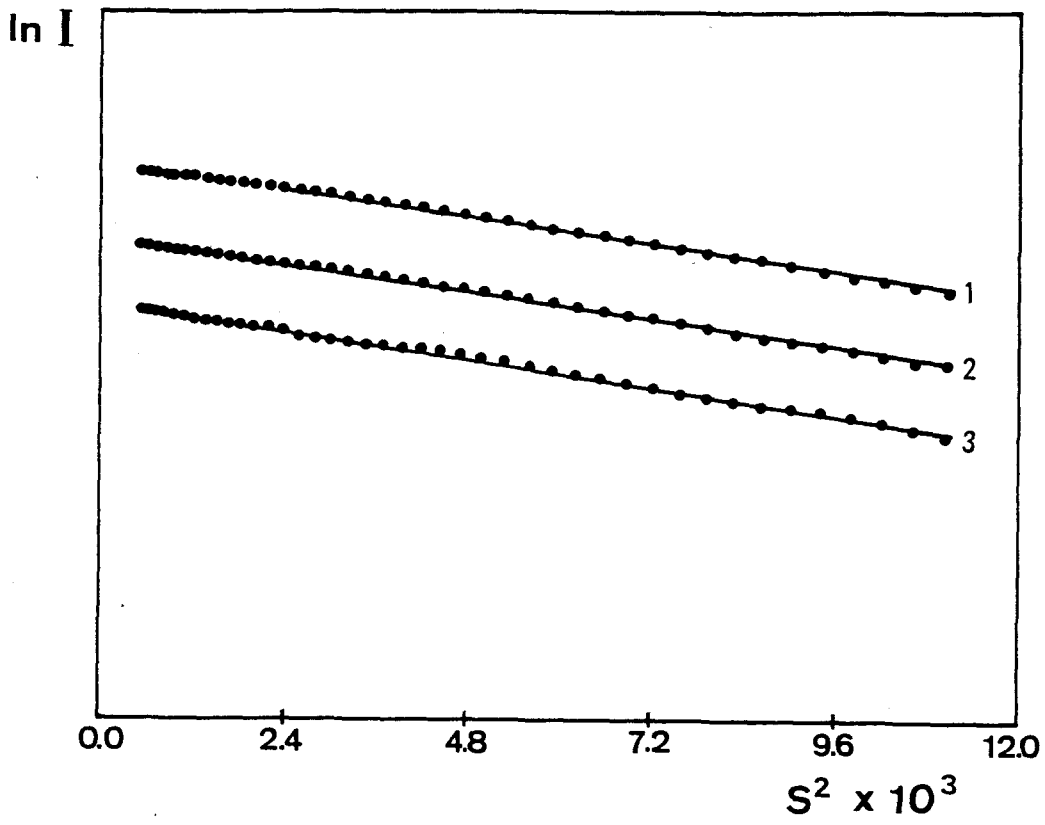

Fig. IV-2. Guinier plots of small-angle X-ray scattering intensities from Taka-amylase A solutions. The protein concentrations of the solutions are 1) 13.2 mg/ml, 2) 10.0 mg/ml and 3) 5.0 mg/ml. The intensity is in arbitrary units.

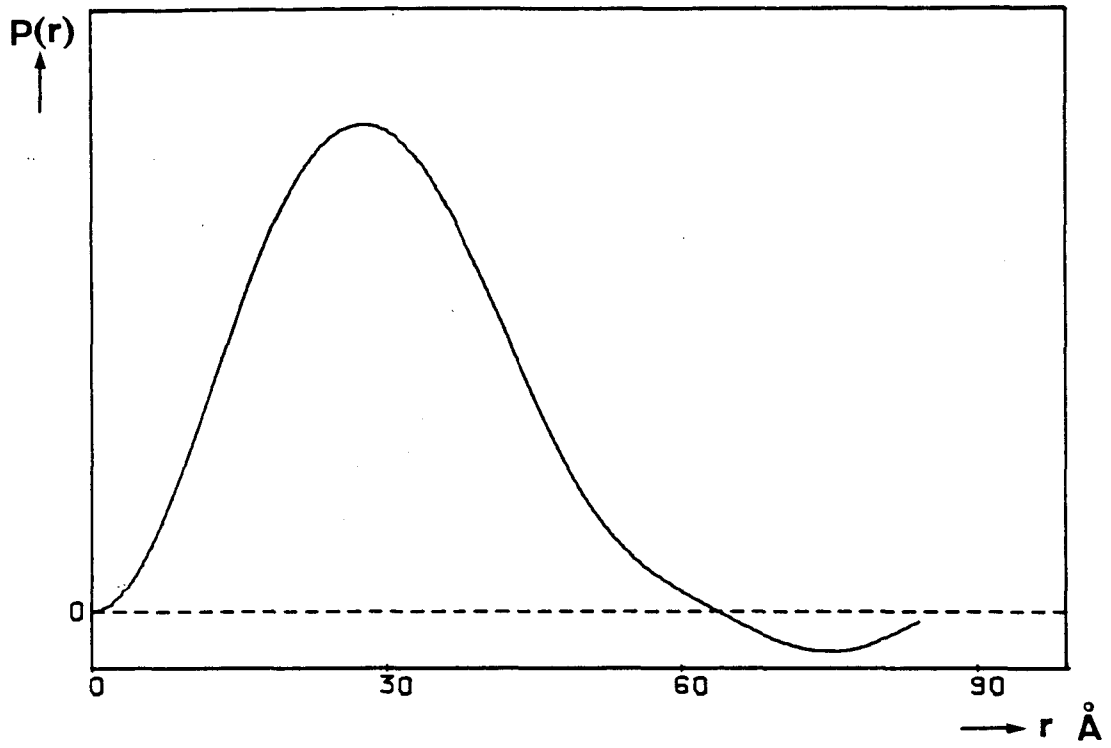

Fig. IV-3. Distance distribution function, $P(r)$ of Taka-amylase A

The molecular weights of Taka-amylase A were determined to be 59 000 and 53 000 from the volumes estimated from the dimensions of the molecule and the scattering intensities, respectively, using the equation [A-10], in which the partial specific volume of Taka-amylase A was determined as 0.70 ml/ g experimentally (51). The molecular parameters of Taka-amylase A are summarized in Table IV-3.

Table IV-3. Molecular parameters of Taka-amylase A

Radius of gyration, R_g	21.0 (Å)
Maximal dimension, D_{max}	65 (Å)
r_{max}	28 (Å)
Molecular volume, V	6.8×10^4 (Å^3) [a]
	6.2×10^4 (Å^3) [b]
Molecular weight, M_r	59 000 [c]
	53 000 [d]

[a] Estimated from the dimensions of an ellipsoid of revolution

[b] Estimated from the small-angle X-ray scattering intensities

[c] Estimated from the volume a)

[d] Estimated from the volume b)

Pseudomonas isoamylase

The precession photographs of the *h 0 l* and *0 k l* zones (Fig. IV-4) showed that *Pseudomonas* isoamylase crystal belongs to the orthorhombic system with unit cell dimensions of a = 137.9 (Å), b = 52.9 (Å), c = 151.2 (Å) and the space group, $P2_12_12_1$. Assuming that the asymmetric unit contains one protein molecule, the V_M and V_{prot} values are 2.90 Å^3/dalton and 0.42, respectively, and these values lie within the range of values usually found for protein crystals (52).
The crystallographic data of *Pseudomonas* isoamylase are summarized in Table IV-4.

Tavle IV-4. Crystallographic data of *Pseudomonas* isoamylase

Crystal system	Orthorhombic
Space group	$P2_12_12_1$
a	137.9 (Å)
b	52.9 (Å)
c	151.2 (Å)
V	1.1 x 10^5 (Å^3)
V_M	2.90 (Å^3/dalton)
V_{prot}	0.42
Z	4

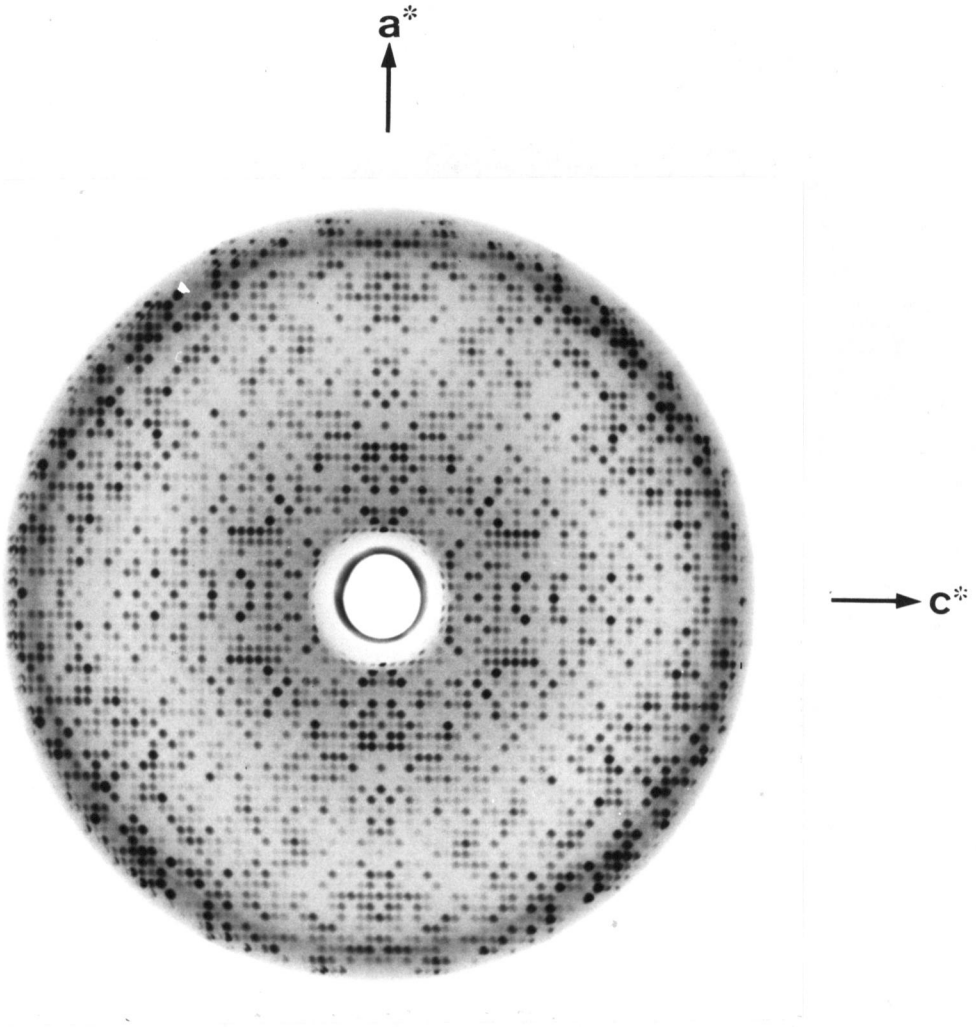

a

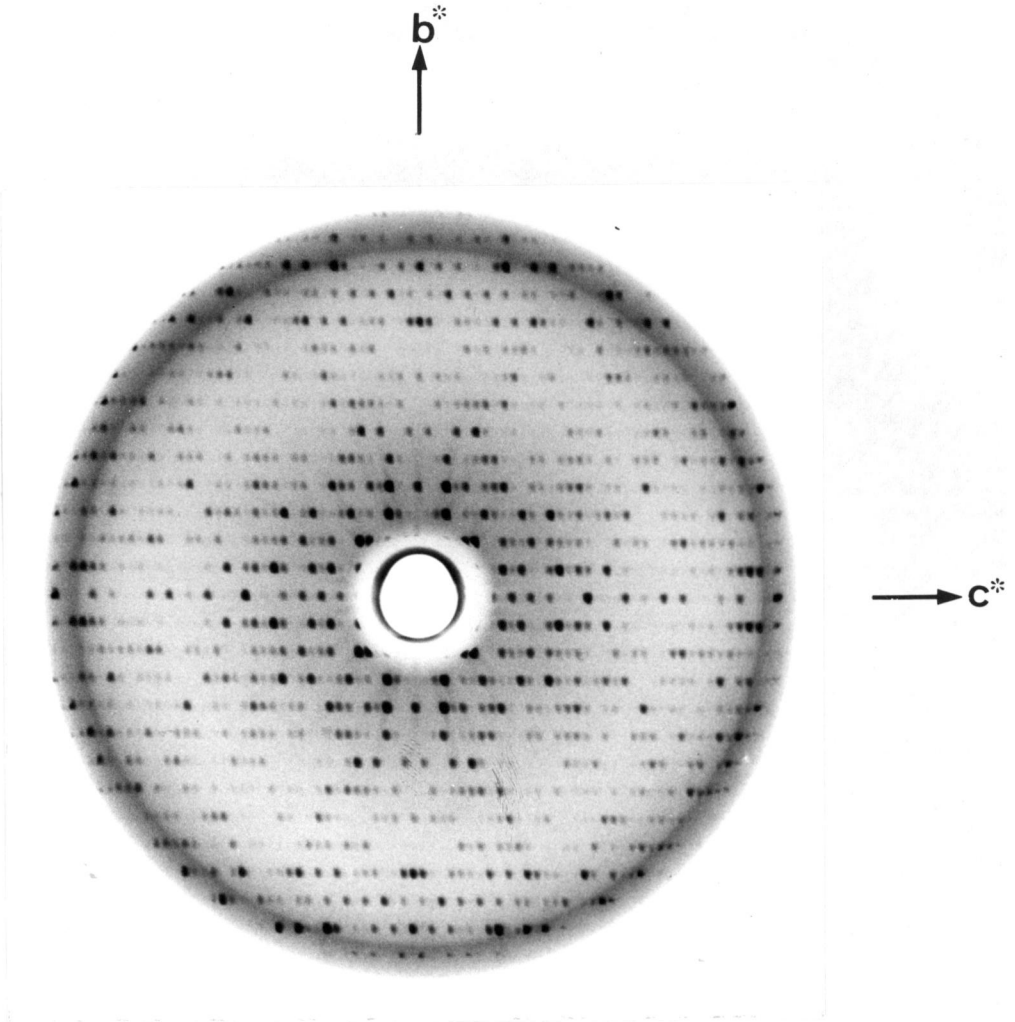

Fig. IV-4. Precession photographs of the *h 0 l* (a) and *0 k l* (b) zones of *Pseudomonas* isoamylase crystal

The small-angle X-ray scattering intensity measurements were carried out on four kinds of *Pseudomonas* isoamylase solutions of the concentrations of 14.6 mg/ml, 10.4 mg/ml, 7.3 mg/ml and 3.6 mg/ml in 10 mM acetate buffer, pH 3.5. Each of the Guinier plots (Fig. IV-5) of the scattering intensities at different protein concentrations was linear within the limits of errors and parallel with each other, which showed no concentration effect (interparticle interference effect) on the observed scattering intensities.

The radius of gyration, R_g of *Pseudomonas* isoamylase was determined to be 27.5 Å from the slope of the Guinier plot. The distance distribution function, $P(r)$ (Fig. IV-6) gave the maximal dimension, D_{max} of *Pseudomonas* isoamylase molecule as 100 Å. Assuming the shape of the molecule as an ellipsoid of revolution with uniform electron density, approximate dimensions of the molecule were estimated to be 50 x 50 x 100 Å by the least-squares fitting between observed scattering intensities and theoretical scattering intensities from an ellipsoid of revolution. The volume of the molecule were determined to be 1.3×10^5 Å^3 and 1.1×10^5 Å^3 from the dimensions of the ellipsoidal molecule and from the small-angle X-ray scattering intensities, using the equation [A-8], respectively. For the determination of Q in the equation, the integration was carried out numerically up to $s = 0.31$ Å^{-1} ($2\theta = 76.7$ mrad) and remaining tail end of the scattering intensity curve was integrated analytically according to Porod (18). The molecular weights of *Pseudomonas* isoamylase were determined to be 108 000 and 91 000 from the volumes estimated from the

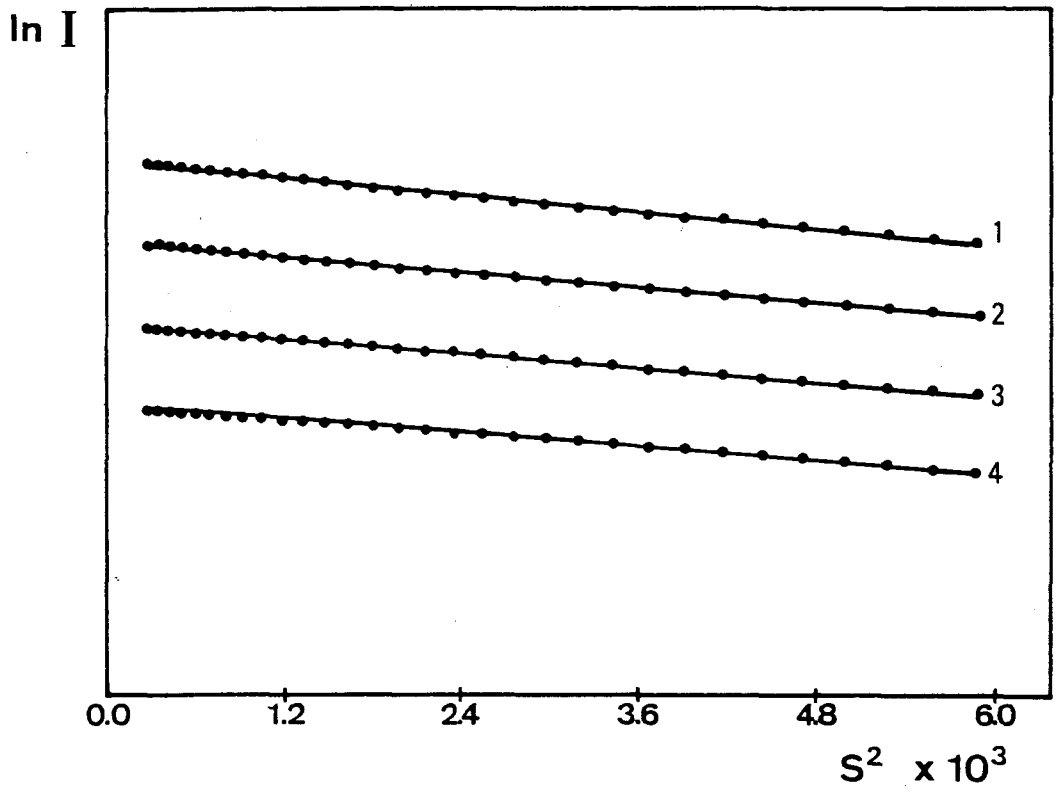

Fig. IV-5. Guinier plots of small-angle X-ray scattering intensities from *Pseudomonas* isoamylase solutions. The protein concentrations of the solutions are 1) 14.6 mg/ml, 2) 10.4 mg/ml, 3) 7.3 mg/ml and 4) 3.6 mg/ml. The intensity is in arbitrary units.

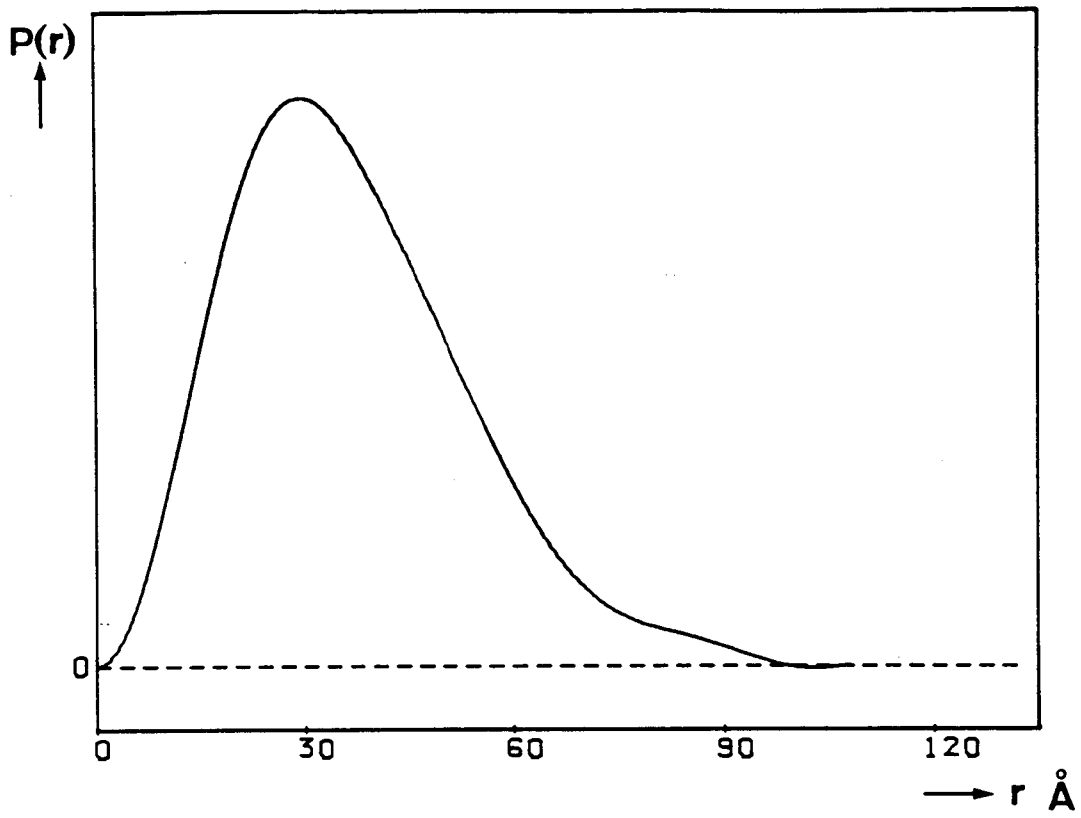

Fig. IV-6. Distance distribution function, $P(r)$ of *Pseudomonas* isoamylase

dimensions of the molecule and the scattering intensities, respectively, using the equation [A-10], in which the partial specific volume of *Pseudomonas* isoamylase was assumed as 0.73 ml/ g. The molecular parameters of *Pseudomonas* isoamylase are summarized in Table IV-5.

Table IV-5. Molecular parameters of *Pseudomonas* isoamylase

Radius of gyration, R_g	27.5 (Å)
Maximal dimension, D_{max}	100 (Å)
r_{max}	29 (Å)
Molecular volume, V	1.3×10^5 (Å^3) [a]
	1.1×10^5 (Å^3) [b]
Molecular weight, M_r	108 000 [c]
	91 000 [d]

a) Estimated from the dimensions of an ellipsoid of revolution

b) Estimated from the small-angle X-ray scattering intensities

c) Estimated from the volume a)

d) Estimated from the volume b)

4. Discussion

Taka-amylase A

The radius of gyration and the maximal dimension of Taka-amylase A have been determined as 21.0 Å and 65 Å, respectively. In addition, the molecule had approximate dimensions of 45 x 45 x 65 Å, assuming the molecule as an ellipsoid. The volumes of the molecule were estimated as 6.8×10^4 Å^3 and 6.2×10^4 Å^3 from the dimensions of the ellipsoid and from the small-angle X-ray scattering intensities, respectively. This agreement in volumes means that the model of the molecule as the ellipsoid is the most plausible one, though the model may not be the unique one as that of Taka-amylase A molecule in solution. The molecular weights of 59 000 and 53 000 estimated from the volumes of the molecule were compatible with the value obtained by the combinated use of high pressure silica gel chromatography and the low-angle laser light scattering method (M_r = 51 000 ± 500 (53)) within the limits of errors.

On the other hand, X-ray diffraction analysis of Taka-amylase A crystal showed that the molecule had an ellipsoidal shape with approximate dimensions of 35 x 45 x 80 Å. From this ellipsoid, the radius of gyration and the volume of the molecule were theoretically calculated to be 22.0 Å and 6.6×10^4 Å^3, respectively, that is, the radius of gyration of the molecule in crystal is 1.0 Å larger than that in solution, followed the same values in the volume of the molecule in crystal and in solution.

The results derived from the small-angle X-ray scattering method and the X-ray diffraction analysis indicate that Taka-

amylase A in solution has the shape more spherical than that in crystal, because the more spherical the molecule is, the smaller the radius of gyration becomes in the molecules with the same volume. This fact is also supported by the distance distribution function with the nearly symmetrical pattern. The change in structures in crystal and in solution may arise from the difference of pH values on crystallization (pH ≃ 7) and of solutions (pH = 4.9) used in the small-angle X-ray scattering intensity measurements. However, judging from the accuracy and the resolution in small-angle X-ray scattering method, the structural change must be ascertained by the precise and systematic measurements of the small-angle X-ray scattering intensities from Taka-amylase A solutions in various pH values.

Pseudomonas isoamylase

The radius of gyration and the maximal dimension of *Pseudomonas* isoamylase have been determined to be 27.5 Å and 100 Å, respectively. In addition, the molecule had approximate dimensions of 50 x 50 x 100 Å, assuming the molecule as an ellipsoid. The volumes of the molecule were estimated to be 1.3×10^5 Å^3 and 1.1×10^5 Å^3 from the dimensions of the ellipsoid and the small-angle X-ray scattering intensities, respectively. This agreement in volumes implies that the model of the molecule as the ellipsoid is most plausible one, though the model may not be the unigue one as that of *Pseudomonas* isoamylase molecule in solution. The molecular weights of *Pseudomonas* isoamylase were determined to be 108 000 and 91 000 from the volumes of the molecule, which were consistent

with the value obtained from Archibald's method (M_r = 95 000, (49)) within the limits of errors.

The precession photographs of the *h 0 l* and *0 k l* zones gave the unit cell dimensions as presented in Table IV-4. On the basis of the unit cell dimensions, the ellipsoidal *Pseudomonas* isoamylase molecule with approximate dimensions of 50 x 50 x 100 Å is expected to be packed in the unit cell of the crystal with the short principal axis (50 Å) along the crystallographic *b*-axis. Taking account of the symmetry of the space group, $P2_12_12_1$, the *Pseudomonas* isoamylase molecule seems to be located in the crystal as shown in Fig. IV-7. The problems about the molecular shape and the packing in crystal will be confirmed according to the progress of crystallographic analysis in future.

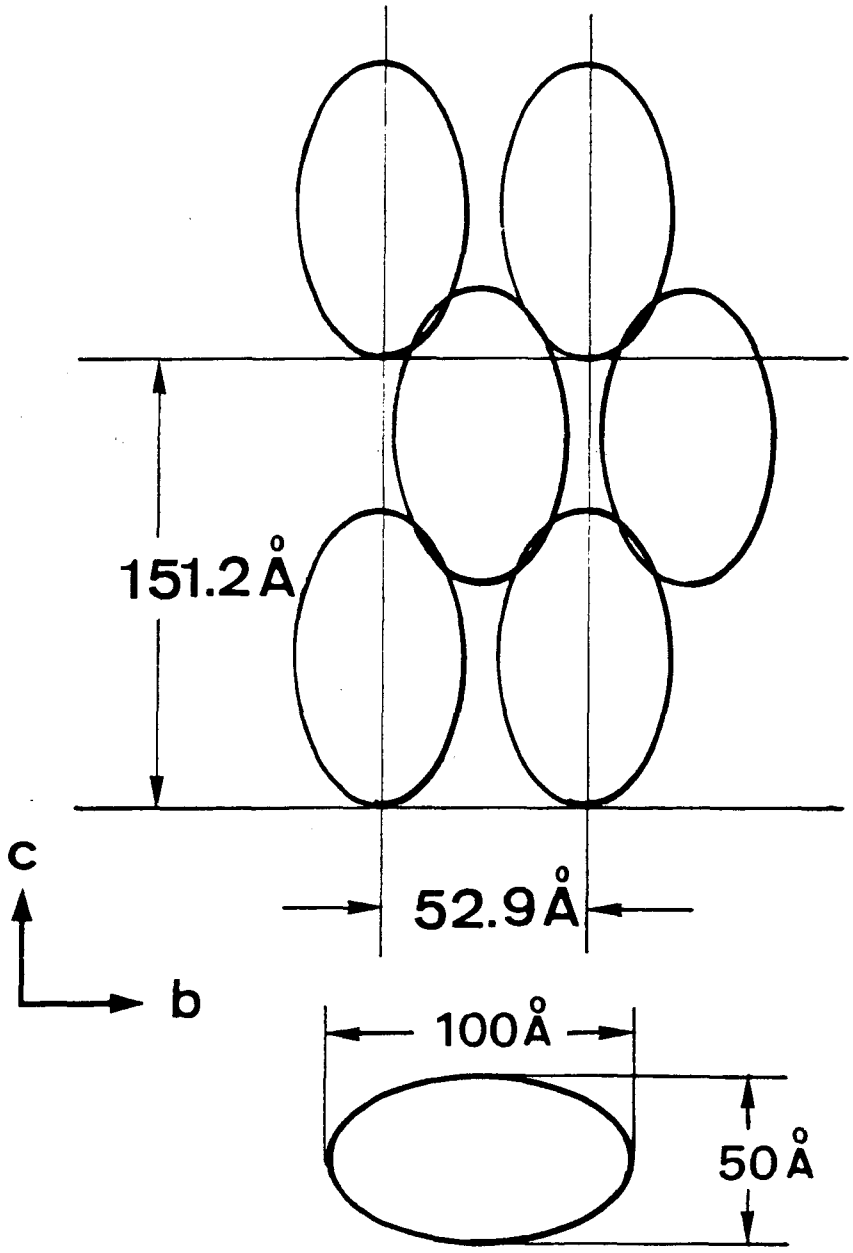

Fig. IV-7. Expected packing aspect of *Pseudomonas* isoamylase in crystal

APPENDIX

Summary of Small-Angle X-Ray Scattering Theory (Explanation of The Parameters Derived from Small-Angle X-Ray Scattering Method)

1. *Radius of gyration,* R_g

The small-angle X-ray scattering intensity, $I(s)$ from a solution containing N particles in irradiated volume may be given by

$$I(s) = PI_eN \int_V \int_V \rho(r_j)\rho(r_k) \frac{\sin sr_{jk}}{sr_{jk}} dv_j dv_k \quad \text{----[A-1]}$$

where s is defined by $s = 4\pi\sin\theta/\lambda$ (2θ : scattering angle, λ : wavelength) , P the intensity of the incident beam, I_e the scattering intensity by one electron at the distance, R from the particle ($I_e = 7.94 \times 10^{-26}/R^2$) and ρ the difference of the electron density between the solute particle and the solvent. The integral with respect to v is carried out over the whole volume of a particle, V. The equation [A-1] is nearly approximated by the Gaussian function in the small-angle region :

$$I(s) = I(0) \exp (- R_g^2 s^2/3) \quad \text{----------[A-2]}$$

where $I(0)$ is the scattering intensity at zero angle ($I(0) = PI_eN\bar{\rho}^2V^2$, $\bar{\rho}$ is the difference of the average electron density between solute and solvent) and R_g the radius of gyration of particle. The radius of gyration, R_g is derived from the slope of the straight line of the log $I(s)$ vs. s^2 plot (Guinier plot)

2. *Maximal dimension of particle, D_{max}*

The "characteristic" function of particle, $\gamma(r)$ (correlation function) has been introduced by Porod (18), which is defined as the three-dimensional convolution square of ρ averaged over all directions in space, that is,

$$\gamma(r) = \frac{1}{4\pi} \int_0^{4\pi} \int_V \rho(\vec{r}_k)\rho(\vec{r}_k + \vec{r})\, dv_k d\omega \quad \text{----------[A-3]}$$

where ω is a solid angle. If the electron density difference, ρ is constant ($\rho = \rho_e$), it follows that

$$\gamma(0) = \frac{1}{4\pi} \int_0^{4\pi} \int_V \rho_e(\vec{r}_k)\rho_e(\vec{r}_k)\, dv_k d\omega$$

$$= \rho_e{}^2 V \quad \text{----------[A-4]}$$

Multiplied to $\gamma(r)$ by r^2, we can obtain the distance distribution function, $P(r)$ (54,55)

$$P(r) = r^2\, \gamma(r)$$

The relation between the distance distribution function, $P(r)$ and the scattering intensity, $I(s)$ is given by (40)

$$P(r) = \frac{1}{2\pi^2} \int_0^{\infty} I(s)(sr)\sin(sr)\, ds \quad \text{----------[A-5]}$$

and the relation between $\gamma(r)$ and $I(s)$ is

$$\gamma(r) = \frac{1}{2\pi^2} \int_0^{\infty} I(s)\, s^2 \frac{\sin(sr)}{sr}\, ds \quad \text{----------[A-6]}$$

The distance distribution function, $P(r)$ multiplied by the factor, 4π represents the number of pairs of difference electrons separated by the distance, r in particle.
The $P(r)$ consequentially gives the information for the maximal dimension of particle, D_{max}, because the function can be different from zero in the range of $0 < r < D_{max}$ and zero for $r \geq D_{max}$. The maximal dimension of particle, D_{max} is given by the r where the $P(r)$ goes down to zero.

3. *Molecular volume, V*

If the electron density difference, ρ is constant ($\rho = \rho_c$), we can obtain the equation :

$$\rho_c^2 = \overline{\rho}^2 = I(0)/(P\ I_e\ V^2) \text{ ----------[A-7]}$$

From the equations [A-4], [A-6] and [A-7], the volume of particle (molecular volume), V is followed to be

$$V = 2\pi^2\ I(0)/\ Q \text{ ----------[A-8]}$$

where Q is the Porod's invariant (18) ($Q = \int_0^\infty I(s)\ s^2\ ds$) and $I(0)$ is the scattering intensity at zero angle, which is determined from extrapolation of s to zero in Guinier plot. However, it is not possible to record the scattering intensity up to $s = \infty$. The integration in the Q is therefore carried out numerically up to the relatively large value of s and remaining tail end of the scattering intensity curve is integrated analytically according to Porod (18).

4. *Molecular weight,* M_r

The molecular weight, M_r of particle (solubilized macromolecule) can be determined from the measurement of $I(0)$ in absolute scale (56,57). The molecular weight, M_r is given by the following equation :

$$M_r = \frac{I(0)}{I_e \; N_A \; P \; (\; z \; - \; \bar{v} \; \rho_0 \;) \; d \; c} \qquad \text{[A-9]}$$

where N_A is the Avogadro's number, z the amount of electrons (in mole) per gram of the solute particle, $\bar{v}$ the partial specific volume of the particle in ml/g, ρ_0 the electron density of the solvent, d the thickness of the sample and c the concentration of the solution.

Another way to obtain the molecular weight, M_r is the use of the volume of the particle, V which is estimated from the equation [A-8] :

$$M_r = \frac{N_A \; V}{\bar{v}} \qquad \text{[A-10]}$$

SUMMARY

Small-angle X-ray scattering method was applied to investigate the structures of cytochrome oxidases and amylases in solution in connection with the function.

CHAPTER I dealed with the small-angle X-ray scattering system that I have developed in order to shorten the measurement and some new treatments of the small-angle X-ray scattering intensity data. The system needed only 10 μl of solution per measurement and could give a significant scattering intensity distribution in the range of scattering angles, 2θ = 4.0 - 76.7 mrad, with 15 - 180 min accumulation of the scattering intensities. The searching of the center of direct X-ray beam so as to minimize a reliability factor made it possible to estimate the accuracy of the scattering intensity data. Correction for collimation effect has been done by the use of a matrix which was uniquely build up from a collimation geometry, the procedure in which was much easier than that in conventional methods.

In CHAPTER II, the structures of cytochrome oxidase isolated from beef heart mitochondria and the complex with cytochrome *c* in solution have been studied. The investigation of the complex formation in various concentrations of buffer showed that cytochrome *c* was bound to the oxidase with an ionic interaction. In the presence of cholate, the oxidase was found to exist as an elongated tetramer with the maximal dimension of 210 Å, which was composed of four structurally minimal units, and bind cytochrome *c* at the top of the elongated one

to form the complex with the maximal dimension of 250 Å.

In CHAPTER III, the structure of cytochrome oxidase isolated from *Nitrobacter agilis* in solution has been investigated in order to characterize its active form. The investigation clarified that, in the presence of nonionic detergent, the oxidase exists as a monomer composed of two subunits and the monomer is an active and functional molecule. In addition, it was shown that the molecule was denaturated by SDS, followed by two kinds of structural changes. The first step of the structural changes was splitting into each subunit and the second was other small structural changes in each subunit such as unfolding of the polypeptide chain.

In CHAPTER IV, the structures of Taka-amylase A and *Pseudomonas* isoamylase in solution and in crystal were discussed. The shape of Taka-amylase A in solution was the ellipsoid with approximate dimensions of 45 x 45 x 65 Å, which was more spherical than that in crystal. The discrepancy between the shapes in solution and in crystal was expected to arise from the difference of pH values on crystallization and of solutions used in the small-angle X-ray scattering intensity measurements. *Pseudomonas* isoamylase crystal belonged to orthorhombic system with the unit cell dimensions of a = 137.9 Å, b = 52.9 Å, c = 151.2 Å and space group of $P2_12_12_1$. The shape of *Pseudomonas* isoamylase in solution was the ellipsoid with approximate dimensions of 50 x 50 x 100 Å, which was expected to be packed in the unit cell of the crystal with the short principal axis along the crystallographic b-axis.

REFERENCES

(1) Kuhlmann, W. R., Lauterjung, K. H., Schimmer, B., and Sistemich, K. (1966) *Nucl. Instrm. Methods* 40, 118

(2) Kratky, O., Porod, G., and Skala, Z. (1966) *Acta phys. Austriaca* 13, 76

(3) Guinier, A. and Fournet, G. (1947) *J. Phys. Radium* 8, 345

(4) DuMond, J. W. M. (1947) *Phys. Rev.* 72, 83

(5) Kratky, O., Porod, G., and Kahovec, L. (1951) *Z. Elektrochem.* 55, 53

(6) Lake, J. A. (1967) *Acta Cryst.* 23, 191

(7) Ozawa, T., Tada, M., and Suzuki, H. (1979) in *Cytochrome Oxidase* (King, T. E., Orii, Y., Chance, B., and Okunuki, K. eds.) Elsevier/ North-Holland, Amsterdam, p. 39

(8) Green, D. E. and Tzagoloff, A. (1966) *J. Lipid Res.* 7, 587

(9) Ozawa, T., Okumura, M., and Yagi, K. (1975) *Biochem. Biophys. Res. Commun.* 65, 1102

(10) Ozawa, T., Suzuki, H., and Tanaka, M. (1980) *Proc. Natl. Acad. Sci. USA* 77, 928

(11) Kawato, S., Sigel, E., Carafoli, E., and Cherry, R. J. (1981) *J. Biol. Chem.* 256, 7518

(12) Gornall, A. G., Bardawill, C. J., and David, M. M. (1949) *J. Biol. Chem.* 177, 751

(13) Yonetani, T. (1961) *J. Biol. Chem.* 236, 1680

(14) Chen, P. S. Jr., Toribara, T. Y., and Warner, H. (1956) *Anal. Chem.* 28, 1756

(15) Fowler, L. R., Richardson, S. H., and Hatefi, Y. (1962) *Biochim. Biophys. Acta* 64, 170

(16) Tzagoloff, A. and MacLennan, D. H. (1965) *Biochim. Biophys. Acta* 99, 476

(17) Hagihara, B., Morikawa, I., Sekuzu, I., and Okunuki, K. (1958) *J. Biochem.* 45, 551

(18) Porod, G. (1951) *Kolloid Z.* 124, 83

(19) Robinson, N. C. and Capaldi, R. A. (1977) *Biochem.* 16, 375

(20) Cohn, E. J. and Edsall, J. T. (1943) *Protein Amino Acid and Peptide* Reinhold Publishing Co., New York

(21) Tanford, C., Nozaki, Y., Reynolds, J. A., and Makino, S. (1974) *Biochem.* 13, 2369

(22) Glatter, O. (1979) *J. Appl. Cryst.* 12, 166

(23) Mittelbach, P. and Porod, G. (1962) *Acta Phys. Austriaca* 15, 122

(24) Tanaka, M. and Ozawa, T. (1982) *Biochem. International* 5, 67

(25) Deatherage, J. F., Henderson, R., and Capaldi, R. A. (1982) *J. Mol. Biol.* 158, 501

(26) Keilin, D. (1966) *The History of Cell Respiration and Cytochromes* Cambridge University Press, London

(27) Morton, R. K. (1958) *Pure and Appl. Chem.* 8, 161

(28) Lemberg, R. and Barrett, J. (1973) *Cytochromes* Academic Press, New York

(29) King, T. E., Orii, Y., Chance, B., and Okunuki, K. (eds.) (1979) *Cytochrome Oxidase* Elsevier/ North-Holland, Amsterdam

(30) Erickson, R. H., Hooper, A. B., and Terry, K. (1972) *Biochim. Biophys. Acta* 283, 155

(31) Yamanaka, T. and Fukumori, Y. (1977) *FEBS Lett.* 77, 155

(32) Yamanaka, T., Fukumori, Y., and Fujii, K. (1979) in *Cytochrome Oxidase* (King, T. E., Orii, Y., Chance, B., and Okunuki, K. eds.) Elsevier/ North-Holland, Amsterdam, p. 399

(33) Yamanaka, T., Fujii, K., and Kamita, Y. (1979) *J. Biochem.* 86, 821

(34) Yamanaka, T. and Fujii, K. (1980) *Biochim. Biophys. Acta* 591, 53

(35) Sone, N., Ohyama, T., and Kagawa, Y. (1979) *FEBS Lett.* 106, 39

(36) Yamanaka, T., Kamita, Y., and Fukumori, Y. (1981) *J. Biochem.* 89, 265

(37) Lowry, O. H., Rosenbrough, N. J., Farr, A. L., and Randall, R. J. (1951) *J. Biol. Chem.* 193, 265

(38) Aleem, M. I. H. and Alexander, M. (1958) *J. Bacteriol.* 76, 510

(39) Hersh, R. T. and Schachman, H. K. (1958) *Virology* 6, 234

(40) Pilz, I., Glatter, O., and Kratky, O. (1979) *Methods in Enzymology* 61, 148

(41) Ludwig, B., Grabo, M., Gregor, I., Lustig, A., Regenass, M., and Rosenbusch, J. P. (1982) *J. Biol. Chem.* 257, 5576

(42) Kamita, Y., Fukumori, Y., and Yamanaka, T., unpublished results.

(43) Matsubara, S., Ikenaka, T., and Akabori, S. (1959) *J. Biochem.* 46, 425

(44) Matsubara, S. (1961) *J. Biochem.* 49, 232

(45) Yamaguchi, H., Ikenaka, T., and Matsushima, Y. (1971) *J. Biochem.* 70, 587

(46) Narita, K. and Toda, H., personal communication

(47) Matsuura, Y., Kusunoki, M., Harada, W., Tanaka, N., Iga, Y., Yasuoka, N., Toda, H., Narita, K., and Kakudo, M. (1980) *J. Biochem.* 87, 1555

(48) Harada, T., Yokobayashi, K., and Misaki, A. (1968) *Appl. Microbiol.* 16, 1439

(49) Yokobayashi, K., Misaki, A., and Harada, T. (1970) *Biochim. Biophys. Acta* 212, 458

(50) Akabori, S., Ikenaka, T., and Hagihara, B. (1954) *J. Biochem.* 41, 577

(51) Isemura, T. and Fujita, S. (1957) *J. Biochem.* 44, 443

(52) Matthews, B. W. (1968) *J. Mol. Biol.* 33, 491

(53) Takagi, T. (1981) *J. Biochem.* 89, 363

(54) Guinier, A. and Fournet, G. (1953) *Small Angle Scattering of X-rays* John Wiley and Sons Ltd., New York

(55) Porod, G. (1948) *Acta Phys. Austriaca* 3, 255

(56) Kratky, O. and Kreutz, W. (1960) *Z. Elektrochem.* 64, 880

(57) Luzatti, V., Witz, J., and Nicolaieff, A. (1961) *J. Mol. Biol.* 3, 367

LIST OF PUBLICATIONS

1. Investigation of The Complex Formation of Cytochrome Oxidase and Cytochrome *c* by Means of Small-angle X-ray Scattering

   Sato, M., Kato, M., Kasai, N., Hata, Y., Tanaka, N., Kakudo, M., Tanaka, M., and Ozawa, T.

   Biochem. International, (1982) 5, 595-602

2. Preliminary X-ray Studies on *Pseudomonas* Isoamylase

   Sato, M., Hato, Y., Ii, Y., Miki, K., Kasai, N., Tanaka, N., and Harada, T.

   J. Mol. Biol., (1982) 160, 669-671

3. Small-Angle X-ray Scattering Studies on Cytochrome aa_3-Type Terminal Oxidase Derived from *Nitrobacter agilis*

   Sato, M., Tanaka, N., Kakiuchi, K., Fukumori, Y., Yamanaka, T., Kasai, N., and Kakudo, M.

   Biochem. International, in contribution